Study of the Function and Dynamics of Myosin II and Actin in Cytokinesis

A Dissertation Presented

By

Mian Zhou

Submitted to the Faculty of the
University of Massachusetts Graduate School of Biomedical Sciences, Worcester
in partial fulfillment of the requirements for the degree of

DOCTOR OF PHILOSOPHY

(May 26th, 2009)

(Interdisciplinary Graduate Program)

STUDY OF THE FUNCTION AND DYNAMICS OF MYOSIN II AND ACTIN IN CYTOKINESIS

A Dissertation Presented By

Mian Zhou

The signatures of the Dissertation Defense Committee signifies completion and approval as to style and content of the Dissertation

Yu-Li Wang, Ph.D., Thesis Advisor

David Burgess, Ph.D., Member of Committee

Stephen Doxsey, Ph.D., Member of Committee

Kirsten Hagstrom, Ph.D., Member of Committee

Greenfield Sluder, Ph.D., Member of Committee

The signature of the Chair of the Committee signifies that the written dissertation meets the requirements of the Dissertation Committee

Dannel McCollum, Ph.D., Chair of Committee

The signature of the Dean of the Graduate School of Biomedical Sciences signifies that the student has met all graduation requirements of the School

Anthony Carruthers, Ph.D.
Dean of the Graduate School of Biomedical Sciences

Interdisciplinary Graduate Program
October 23, 2008

Copyright Notice

Acknowledgements

I would like to thank Dr. Yu-Li Wang and all the people from Wang lab, for their support, encouragement and helpful discussion. I would like to thank Dr. Alonzo Ross and Dr. Dannel McCollum, for their help and encouragement during my lab rotations. I also would like to thank people from the Biotech Four Building and School campus for their help. Lastly, I would like to thank my husband, my family and my friends for their love and support.

Abstract

Myosin II and actin are two major components of the ingressing cortex during cytokinesis. However, their structural dynamics and functions during cytokinesis are still poorly understood. To study the role of myosin II in cortical actin turnover, dividing normal rat kidney (NRK) cells were treated with blebbistatin, a potent inhibitor of the non-muscle myosin II ATPase. Blebbistatin caused a strong inhibition of actin filament turnover and cytokinesis. Local release of blebbistatin at the equator caused inhibition of cytokinesis, while treatment in the polar region also caused a high frequency of abnormal cytokinesis, suggesting that myosin II may play a global role. These observations indicate that myosin II ATPase is essential for actin turnover and remodeling during cytokinesis.

To further study the mechanism of myosin II and actin recruitment to the cytokinetic furrow, equatorial cortex were observed with total internal reflection fluorescence microscope (TIRF-M) coupled with spatial temporal image correlation spectroscopy (STICS) and a new approach termed temporal differential microscopy (TDM). The results indicated at least partially independent mechanisms for the early equatorial recruitment of myosin II and actin filaments. Cortical myosin II showed no detectable directional flow toward the equator. In addition to de novo equatorial assembly, localized inhibition of disassembly appeared to contribute to the formation of the equatorial myosin II band. In contrast, actin filaments underwent a striking, myosin II dependent flux toward the equator. However, myosin II was not required for equatorial actin concentration, suggesting that there was a flux-independent, de novo mechanism.

The study was then extended to retraction fibers found typically on mitotic adherent cells, to address the hypothesis that they may facilitate post-mitotic spreading. Cells with

retraction fibers showed increased spreading speed in post-mitotic spreading compared to cells without retraction fibers. In addition, micromanipulation study suggested that retraction fibers may guide the direction of post-mitotic spreading. Focal adhesion proteins were present at the tips of retraction fibers, and may act as small nucleators for focal adhesions reassembly that help cell quickly respread and regrow focal adhesions. These findings may suggest a general mechanism utilized by adherent cells to facilitate post-mitotic spreading and reoccupy their previous territory.

Table of Contents

List of Figures

Chapter I - Introduction

Cytokinesis, the last step of cell division that divides the cytoplasm of a mother cell into two daughter cells, is a fascinating phenomenon to many scientists. The study of cytokinesis began in the very early era of cell biology, yet many mysteries remain unanswered. The whole process of cytokinesis can be arbitrarily divided into four sequential steps. First, following chromosome segregation, the cell specifies the future site of cytokinetic ingression. Second, a cleavage furrow and a band of cortical acto-myosin structure forms at the specified ingression site, also referred to as contractile ring assembly. This is followed by the third step, the continuous ingression of the furrow that divides mother cell into two daughter cells. The two daughter cells however remain connected by a thin strand of membrane and cytoplasm, called midbody. The final step, abscission, may take several hours to finish. There does not appear to be clear-cut gaps between these steps. For example, ingression of the furrow may take place before the assembly of contractile ring ends.

During the last two decades, the cytokinesis field has seen an explosion of interest and rapid acquisition of knowledge. The current status of cytokinesis research has been expertly reviewed by many scientists (McCollum, 2004; Burgess and Chang, 2005; Matsumura, 2005; Piekny *et al.*, 2005; Wang, 2005; Wolfe and Gould, 2005; Eggert *et al.*, 2006; Barr and Gruneberg, 2007). In this introduction chapter, I will first describe our current knowledge of cytokinesis, mainly focusing on the mechanisms of positioning of the division site, the assembly of the equatorial cortex, and ingression of the equatorial cortex, subjects closely related to my thesis research. At the end of the introduction

chapter, I will also discuss our current understanding of post-mitotic spreading in relation to retraction fibers, which is related to the third part of my thesis research.

Specification of cleavage plane by microtubules

While most cell types divide near the middle, partitioning the cytoplasm equally into two daughter cells, there are exceptions such as asymmetrical division during embryonic development. Specification of the cleavage plane appears to be finely controlled, ensuring that each daughter cell receive a single copy of the genome. How a cell chooses its future division site is the first important question facing scientists.

Early studies of cytokinesis are marked by a series of elegant, insightful experiments to address this question. It is known that the mitotic spindle positions the future division site and microtubules play a key role. However, which parts of the mitotic spindle are involved and how they specify the cleavage plane are still unclear (Rappaport, 1996).

Microtubules of the mitotic spindle can be classified into four categories according to their relative location during anaphase (Burgess and Chang, 2005). The spindle midzone or central spindle refers to the structure that forms in the center of the spindle and consists of overlapping antiparallel microtubules. Kinetochore microtubules are the microtubules emanating from centrosomes that attach to the chromosomes at kinetochores. Astral microtubules are microtubules outside these regions, extending from spindle poles toward the cortex. According to where they touch the cortex, they can be further categorized as polar astral microtubules and equatorial astral microtubules.

The first question to discuss is which set of microtubules is able to induce furrow formation. Early studies conducted by Rappaport in echinoderm eggs suggested that

overlapping astral microtubules may induce furrow formation at sites without chromosomes and spindle midzone (Rappaport, 1961); the ectopic furrow is well known as the “Rappaport furrow”. This idea is supported by micromanipulation experiments, which show that physically removing chromosomes or spindle midzone does not inhibit furrow initiation (Hiramoto, 1971). However, later studies suggest that astral microtubules may not be essential for furrow positioning, and that the spindle midzone plays a more important role (Cao and Wang, 1996; Wheatley and Wang, 1996; Bonaccorsi *et al.*, 1998; Basto *et al.*, 2006). This apparent discrepancy is speculated to be related to the different sizes of organisms under study. For example, in embryo cells, astral microtubules may play a major role because the spindle midzone is too far from the cell cortex due to the large size of the cell. In contrast, in smaller cells like cultured somatic cells, spindle midzone may play a bigger role due to the proximity of the cortex. A recent reinvestigation of this old question, however, points to a new model suggesting that normal furrowing requires inputs from both the astral microtubules and spindle midzone. These signals are temporally distinct and work consecutively to initiate and enforce furrow formation (Bringmann and Hyman, 2005). Thus, it is likely that most cells receive signals from both astral and midzone microtubules to initiate and complete furrowing, and that the previous discrepancies may originate from the observations of extreme circumstances.

The second question concerns the nature of the signals transmitted to the cortex by the microtubules and how microtubules transmit the signals. Is it a stimulating signal or inhibitory signal? Is the signal triggered by microtubule bundling, microtubule density or microtubule dynamics? These questions have been discussed since the early theories of

cytokinesis. The equatorial stimulation model proposes that a positive signal is imparted to the equatorial cortex by microtubules for the formation of cleavage furrow. In contrast, the polar relaxation model states that a negative signal is transmitted to the polar cortex to inhibit cortical tension in the pole region, which results in a net increase of cortical tension in the equatorial region. Experiments conducted by Rappaport argue against the polar relaxation model (Rappaport, 1996). For example, by manipulating the cells he demonstrates that cells can form a furrow without astral microtubules touching the polar cortex (Rappaport, 1960, 1968). The polar relaxation model is supported by mathematical modeling and observations that microtubules appear to inhibit the contractile activity of cell cortex (White and Borisy, 1983; Severson and Bowerman, 2003). In cells with shortened or disrupted microtubules, the cortex appears to be more contractile and forms pseudo-furrows (Severson and Bowerman, 2003). The polar relaxation model was also used to explain the assembly of cytoskeletal components along the furrow (White and Borisy, 1983). Although the discovery of an increasing number of molecules accumulating in the equatorial region (discussed later), in contrast to the poorly defined nature of the negative signals imparted to polar cortex, appears to favor overwhelmingly the equatorial stimulation model over polar relaxation model, these two models may not be mutually exclusive. It is hard to imagine a cell undergo such a dramatic morphological change during cytokinesis without remodeling the polar cortical structure and cortical tension. The observation of increased blebbing activities on the polar cortex during anaphase may suggest an increase of pressure inside the cell, and the polar cortex may respond to this pressure by weakening the cortical tension to facilitate the furrowing activities in the equatorial region. Cytokinesis could be a complicated process that

requires reorganization of cortical structure and tension both in the equatorial and polar region.

How do microtubules direct the signals to the cortex? There are numerous relevant observations and speculations. Overlapping of astral microtubules was thought to be a requisite as suggested by the Rappaport furrow. However, monoastral microtubules were shown to be able to induce furrow formation without overlapping microtubules (Canman *et al.*, 2003). A regulatory mechanism involving different microtubule density in the equatorial and polar region seems also to lack solid evidence. Similarly, microtubule dynamics were proved to be nonessential for furrow initiation (Shannon *et al.*, 2005; Strickland *et al.*, 2005). It appears none of these properties of microtubule are strictly required for transmitting the signal to the cortex. More likely, it is some molecules associated with microtubules, not the microtubule itself, which determine the ability to transmit signals.

In summary, both spindle midzone and astral microtubules are able to deliver signals to the equatorial region. In most cell types, they may work together to initiate and complete furrowing. Their relative importance in furrow positioning may be related to cell types or cell sizes. Whether the nature of the signals they transmitted is similar or distinct is still unclear.

Molecular mechanism in cleavage furrow formation in cytokinesis

Over a hundred molecules have been found to localize in the equatorial region, but little is known about the function of most of them. The small GTPase Rho is believed to be heavily involved in cleavage furrow formation (Piekny *et al.*, 2005). Experiments

inhibiting Rho activity through C3 transferase treatment or depletion of RhoA disrupt cortical contractility or furrow formation, suggesting that Rho activity is required for cytokinesis (Kishi *et al.*, 1993; Mabuchi *et al.*, 1993; Drechsel *et al.*, 1997; O'Connell *et al.*, 1999; Prokopenko *et al.*, 1999; Tatsumoto *et al.*, 1999; Jantsch-Plunger *et al.*, 2000; Yuce *et al.*, 2005). The known effectors of RhoA include Rho-dependent kinase (ROCK), Citron kinase and members of the formin family. ROCK is able to phosphorylate regulatory myosin light chain (rMLC) on Ser19 both in vitro and in vivo (Amano *et al.*, 1996; Kosako *et al.*, 2000; Piekny and Mains, 2002; Royou *et al.*, 2002). ROCK also increases myosin phosphorylation through inhibiting myosin phosphatase (Kimura *et al.*, 1996). Phosphorylation of rMLC on Ser19 leads to increased myosin assembly and contractility. Inhibition of ROCK activity by ROCK inhibitors or genetic depletions causes delay in furrow ingression, suggesting that ROCK is required for cytokinesis (Madaule *et al.*, 1998; Kosako *et al.*, 2000). However ROCK is not the only kinase able to phosphorylate rMLC and regulate myosin contractility during cytokinesis. Citron kinase, another effector of RhoA, is also able to phosphorylate rMLC at Ser19 and Thr18 (Yamashiro *et al.*, 2003). However, citron kinase seems to act at the late stage of cytokinesis, and depletion of citron kinase causes furrow regression (Echard *et al.*, 2004; Naim *et al.*, 2004). Formin, another important effector of RhoA, is involved in actin polymerization during cytokinesis (Goode and Eck, 2007). Activated RhoA binds formin, relieves the autoinhibition of formin and promotes actin polymerization (Watanabe *et al.*, 1999; Alberts, 2001). By regulating both myosin and actin polymerization, RhoA potentially regulates actomyosin ring assembly and its contractility during cytokinesis.

How is RhoA activity regulated during cytokinesis? Rho activity is generally regulated by GEF (GDP-GTP exchange factor) that promotes GTP binding, and GAP (GTPase activating factor) that promotes GTP hydrolysis. The RhoGEF ECT2 is an upstream activator of RhoA (Prokopenko *et al.*, 1999; Glotzer, 2005). RhoA activity appears to be spatially and temporally regulated during cytokinesis. Active RhoA concentrates on the equatorial cortex before furrow ingression and its localization appears to depend on microtubules (Bement *et al.*, 2005). At late stage of furrowing, RhoA activity is reported to be turned off by a RhoGAP, CYK4/MgcRacGAP (Jantsch-Plunger *et al.*, 2000; Minoshima *et al.*, 2003). It is less clear how microtubules deliver the signals and confine the RhoA activation to a narrow zone at the site of future furrow formation. One possibility is transportation of signals along microtubules through motors, such as kinesin.

Other proteins involved in cleavage furrow formation include chromosome passenger complex (CPC) proteins, which are composed of Aurora B kinase and three non-enzymatic subunits, the inner centromere protein (INCENP), survivin and borealin. The CPC proteins got their name because of their very dynamic localization during mitosis. They first localize at the inner centromeric chromatin during prometaphase, then relocalize to the midzone microtubules and sub-equatorial cortex at the anaphase onset, and finally concentrate in the midbody toward the end of cytokinesis. The CPC proteins have various important functions in mitosis, including regulation of kinetochore attachment and chromosome segregation, and controlling the spindle checkpoint, mitotic chromosome structure and spindle formation (Andrews *et al.*, 2003; Vader *et al.*, 2006; Ruchaud *et al.*, 2007). In addition, the CPC proteins are also involved in cytokinesis.

They associate with the antiparallel microtubules in the midzone and equatorial cortex of the future division site before the formation of cleavage furrow, consistent with a role in cleavage site specification (Earnshaw and Cooke, 1991; Eckley *et al.*, 1997). Perturbation of the activities of CPC proteins also leads to various defects in cytokinesis (Ruchaud *et al.*, 2007). However, because of the multiple roles of CPC proteins in both mitosis and cytokinesis, it is difficult to dissect the specific role of CPC proteins involved in cytokinesis. The localization of CPC proteins appears to be regulated by Cdk1 and Cdc14 phosphatases (Pereira and Schiebel, 2003; Gruneberg *et al.*, 2004). There are two known Aurora B substrates in cytokinesis, the MgcRacGAP and the kinesin MKLP/Zen4 (Minoshima *et al.*, 2003; Guse *et al.*, 2005). Aurora B mediated phosphorylation of MgcRacGAP/CYK-4 appears to be required for the completion of cytokinesis (Minoshima *et al.*, 2003). In addition, Aurora B can phosphorylate the MKLP1 homologue Zen4 in C.elegans, while non-phosphorylable Zen4 mutants have defects in the completion of cytokinesis (Piekny *et al.*, 2005). These two substrates form a complex termed centralspindlin, which is important for spindle assembly and cytokinesis (Piekny *et al.*, 2005). However, additional substrates of Aurora B remain to be discovered, and the connection between CPC proteins and activation of RhoA pathway remain to be further elucidated. Another important kinase involved in cytokinesis is polo-like kinase 1 (Plk1). It has been recently demonstrated that Plk1 activity is required for the recruitment of RhoA GTP exchange factor ECT2 to the central spindle, while inhibition of Plk1 leads to disruption of RhoA localization and cleavage furrow formation (Burkard *et al.*, 2007; Lowery *et al.*, 2007; Petronczki *et al.*, 2007; Ruchaud *et al.*, 2007).

Compared with the elusive nature of astral microtubules, the molecular mechanism involved in spindle midzone assembly is better understood. The formation of spindle midzone requires the function of bundling protein such as PRC1, and kinesins such as MKLP1 (Glotzer, 2003). PRC1 bundles microtubules in vitro and in vivo, and appears to be regulated by Cdk1 activity (Mollinari *et al.*, 2002). MKLP1 is a plus-end-directed motor protein that cross-links microtubules (Nislow *et al.*, 1992), possibly under the regulation of Cdk1 (Mishima *et al.*, 2004). Cdk1 phosphorylation appears to negatively regulate both the bundling activity of PRC1 (Jiang *et al.*, 1998; Mollinari *et al.*, 2002) and motor activity of MKLP1 (Gruneberg *et al.*, 2004). Loss of function of PRC1 and MKLP1 results in the disruption of spindle midzone assembly (Mollinari *et al.*, 2005). Another factor involved in spindle midzone assembly is centralspindlin that consists of a Rho family GAP, CYK-4/MgcRacGAP and the kinesin ZEN-4/MKLP1 (Glotzer, 2003), which colocalize with CPC proteins including Aurora B at the spindle midzone. ZEN-4/MKLP1 and CYK-4/MgcRacGAP are both known substrates for Aurora B, and Aurora B mediated phosphorylation of centralspindlin complex appears to be required for the completion of cytokinesis. Interactions among these players are likely to be complex and remain to be further elucidated.

Assembly of the equatorial cortex – the contractile ring hypothesis

It is known that actin, myosin and other proteins accumulate at the equatorial region during cytokinesis (Satterwhite and Pollard, 1992). The classical model of cytokinesis is often referred as the contractile ring hypothesis where actin and myosin II filaments assemble into contractile bundles around the equatorial cortex like a ring structure.

Sliding of anti-parallel actin filaments, powered by the motor activity of myosin, shortens the actin filament bundles and leads to the contraction of the ring (Schroeder, 1972). While this model is very comprehensible in a way that is similar to the contraction of muscle myofibrils, there is still no direct evidence and the exact structure of the actomyosin filaments is still a mystery. As reviewed by Mitchison, there are several possible alignments of actomyosin filaments in the equatorial region other than the "purse-string" model (Eggert *et al.*, 2006). For example, actin filaments could connect the dorsal part of the furrow to the ventral surface, as suggested by some structural studies (Fishkind and Wang, 1993). In this way, the contractile force is directed inward. Other observations of fluorescently-labeled actin filaments suggest a different organization of actin filaments, as they align parallel to the cortex in the longitudinal direction (DeBiasio *et al.*, 1996; Oegema *et al.*, 2000; Dean *et al.*, 2005), which produces no inward force. It is also possible that actomyosin filaments could be poorly organized or organized as a mixture of the configurations mentioned above, while still capable of generating forces (Eggert *et al.*, 2006). A recent study in yeast cells revealed a more detailed picture of the actomyosin alignments (Kamasaki *et al.*, 2007). Further investigation of the structure in mammalian cells is needed and will help to explain the mechanism of force generation.

Despite the lack of information about the three-dimensional structure of actomyosin ring, there are more studies of the equatorial assembly of actin and myosin. One question is how myosin and actin accumulate in the equatorial region. The recruitment of actin in the equatorial region could involve direct nucleation in the furrow or transport from elsewhere to the furrow. The transportation hypothesis is favored by the cortical flow model, as supported by imaging actin filament using a combination of fluorescence

labeling and micromanipulation (White and Borisy, 1983; Cao and Wang, 1990a). Direct observation of the flow of actin filaments to the equatorial region further supports this hypothesis (Cao and Wang, 1990a; Hird and White, 1993; Murthy and Wadsworth, 2005). Cortical flow is an interesting phenomenon that involved in various biological functions such as wound closure, migration and cytokinesis. It can be visualized as the movement of small beads attached to the membrane and sub-membrane cortical structures (Wang *et al.*, 1994). However, the underlying mechanism of cortical flow remains to be further elucidated.

The actin de novo assembly hypothesis is supported by probing the roles of formins and Arp2/3. Formins are a group of proteins that promote rapid assembly of actin filaments (Goode and Eck, 2007). Unlike Arp2/3, formins are believed to nucleate linear unbranched actin filaments such as stress fibers. The common feature of all formin proteins is a FH2 domain that mediates the assembly of actin filaments. There are multiple formin genes in eukaryotic species. Mammals have 15 formin genes (Goode and Eck, 2007), among which the most studied are diaphanous-related formins (DRF). The C-terminal half of DRF is the actin assembly domain, and the N-terminal half is the regulatory domain that mediates the intramolecular interactions with the C terminus to maintain the formins in an autoinhibited state (Goode and Eck, 2007). This autoinhibited state is released by association with activated Rho proteins (Watanabe *et al.*, 1999; Alberts, 2001). During cytokinesis, active RhoA localizes to the equatorial regions and functions as a potential regulator to promote actin assembly through formin activation. In addition, the role of formins in cytokinetic furrow assembly is supported by several lines of evidence (Castrillon and Wasserman, 1994; Chang *et al.*, 1997; Imamura *et al.*, 1997;

Severson *et al.*, 2002; Tolliday *et al.*, 2002; Ingouff *et al.*, 2005). Perturbation of formin function leads to defects in furrow assembly and cytokinesis failure (Castrillon and Wasserman, 1994; Severson *et al.*, 2002). However, the exact role of formins in cytokinesis needs further clarification, for example, whether they act exclusively in the equatorial region, or nucleate actin elsewhere followed by transport to the equator. The Arp2/3 complex is a different set of actin nucleator that generates new actin filaments as branches on existing actin filaments, such as the actin network in the lamellipodium of a migrating cell. It is thought that Arp2/3 complex is not essential for cytokinesis in many species (Hudson and Cooley, 2002; Pelham and Chang, 2002; Severson *et al.*, 2002; Tolliday *et al.*, 2002). However, in the absence of formin function, S.pombe Arp2/3 becomes essential for contractile ring formation, suggesting that Arp2/3 plays at least an indirect role (Pelham and Chang, 2002). In summary, the actin transportation hypothesis and de novo assembly hypothesis are likely non-mutually exclusive as evidence for both are quite strong. Future investigations are required to determine their relative contributions to actin ring assembly and the associated regulatory mechanism.

Nonmuscle myosin II is another major component of the contractile ring. Myosin II is a hexamer composed of two heavy chains, two essential light chains and two regulatory light chains. Each heavy chain has a globular head domain that contains the actin and ATP binding site, and an α-helical coiled coil domain (the rod) that is responsible for self assembly. The essential and regulatory light chains bind to the head domain and regulate both the motor activity and self assembly (Scholey *et al.*, 1980; Bresnick, 1999). There are at least three myosin II homologues in vertebrate cells, myosin IIA, IIB and IIC (Simons *et al.*, 1991; Phillips *et al.*, 1995; Golomb *et al.*, 2004),

among which myosin IIA and IIB are well studied and both localize in the cytokinesis furrow. They appear to have redundant functions, as knock-out either one of them causes no obvious cytokinesis failure (Takeda *et al.*, 2003; Conti *et al.*, 2004). However, they may have different emphases in cellular functions as suggested by their differential localizations and loss-of-function phenotypes in interphase cells (Maupin *et al.*, 1994; Kolega, 1998; Even-Ram *et al.*, 2007). The motor activity and filament assembly of myosin II are regulated by phosphorylation of rMLC at Ser19/Thr18 (Moussavi *et al.*, 1993). The major phosphorylation site is Ser19, while di-phosphorylation at both Ser19 and Thr18 further promotes filament assembly (Ikebe *et al.*, 1988). A recent study in sea urchin eggs shows that mono-phosphorylated rMLC is concentrated in the equaotrial region before cleavage of the furrow and throughout the whole process of cytokinesis, while di-phosphorylated rMLC is detected only after cleavage of the furrow and is much less in quantity than mono-phosphorylated rMLC, suggesting that mono-phosphorylated rMLC is the main active form of myosin in cytokinesis (Uehara *et al.*, 2008). Multiple evidence suggest that myosin regulatory light chain phosphorylation is crucial for actomyosin ring assembly and furrow contraction (Jordan and Karess, 1997; Komatsu *et al.*, 2000). At least three kinases capable of phosphorylating rMLC, ROCK, myosin light chain kinase (MLCK) and citron kinase , are known to localize in the cytokinetic furrow(Madaule *et al.*, 1998; Kosako *et al.*, 2000; Chew *et al.*, 2002). The function of ROCK and citron kinase are regulated by RhoA pathway as discussed in previous sections. MLCK is regulated differently by Ca2+/calmodulin (Gallagher *et al.*, 1991). Florescence resonance energy transfer (FRET) study indicates that MLCK is activated at the equator immediately before the contraction of the cleavage furrow (Chew *et al.*,

2002), while inhibition of MLCK activity by ML-7 relaxes furrow contraction (Murthy and Wadsworth, 2005), suggesting that MLCK regulates myosin contractility in cytokinesis. The role of MLCK and ROCK in rMLC phosphorylation needs further investigation as new observations surface. In compressed sea urchin eggs it is reported that MLCK is required for the initiation of a global myosin II based contractility during metaphase-anaphase transition and the subsequent cytokinesis, while ROCK is not required for the prefurrow contractility but is required for the furrowing because H1152, a ROCK inhibitor, inhibits furrowing (Lucero *et al*., 2006). Another study in sea urchin eggs confirms the role of MLCK as inhibition of MLCK decreases rMLC mono-phosphorylation and blocks contractile ring formation. However, it is found that ROCK is not involved in rMLC phosphorylation because Y27632, a ROCK inhibitor, has no effect in rMLC mono-phosphorylation and cell division (Uehara *et al***.**, 2008). The discrepancy may be due to the different chemicals used to inhibit ROCK. rMLC phosphorylation is also regulated by myosin phosphatase, MYPT1, that appears to function in cytokinesis in C.elegans (Piekny and Mains, 2002). In addition to its role in regulating myosin phosphorylation, MYPT1 may decrease phosphorylation of polo-like kinase 1 (PLK1) at its activating site, thus antagonizing PLK1 activity (Yamashiro *et al*., 2008).The motor activity of myosin II is not required for its recruitment to the cytokinetic furrow, as suggested by experiments using truncated myosin proteins or drugs that inhibit its motor activity (Zang and Spudich, 1998; Straight *et al.*, 2003; Guha *et al.*, 2005). As for actin, these results raise the question whether myosin II is recruited to the cytokinetic furrow by cortical flow, de novo self-assembly or association with equatorial cortex mediated by other molecules. Recent evidence suggest that myosin II recruitment and its maintenance

of localization may involve multiple pathways that require rMLC phosphorylation, actin assembly and some proteins localized to the furrow such as anillin (Dean *et al.*, 2005). It is worth noting that in fission yeast the mechanism of myosin II recruitment may be different from that in mammalian cells, as myosin II is present in the medial plate as precursor dot-like structures before the assembly of actomyosin ring (Feierbach and Chang, 2001; Hou and McCollum, 2002).

The assembly of equatorial cortex involves not only actin and myosin II assembly, but also many other proteins that help to regulate and maintain this contractile structure. For example, septins are filament-forming GTPases that assemble into two rings on either side of the contractile ring and may help to restrict the position of the contractile ring (Dobbelaere and Barral, 2004), anillin is thought to help stabilize the contractile ring and restrict the spreading of the cleavage furrow (Oegema *et al.*, 2000; Straight *et al.*, 2005), while α-actinin is an actin cross-link protein involved in regulating contractile ring dynamics (Mukhina *et al.*, 2007).

Ingression of equatorial cortex in cytokinesis

The mechanical mechanism of cortical ingression in early cytokinesis is still under debate (Wang, 2005). The classic "purse-string" model argues that the tightening of the purse-string causes the equatorial cortex to ingress. This mechanical model is supported by the increase in equatorial cortical rigidity during ingression (Rappaport, 1996; Matzke *et al.*, 2001), and by the presence of inward forces (Rappaport, 1967). However, these experiments are far from conclusive and could be explained in alternative ways (Wang, 2005). Several lines of evidence point to a more complex picture of force distribution on

the cortex and potential alternative mechanisms of cortical ingression during cytokinesis. Micromanipulation and local drug treatment studies conducted indicated that local release of cytochalasin D (an actin disrupting agent) near the equator not only fails to inhibit cytokinesis but appears to increase the rate of ingression. To the contrary, release of cytochalasin D near the polar cortex inhibits cytokinesis (O'Connell *et al.*, 2001). These results suggest that cortical integrity is regulated over a wide area for cytokinesis, and that weakening of the equatorial cortex may facilitate ingression (Wang, 2005). Traction forces exerted by two daughter cells trying to migrate away from each other during late cytokinesis may be an alternative mechanism specific for migrant and adhesive cells (Wang, 2005). This model is supported by the observation that adherent mammalian cells are able to ingress in the middle without actomyosin concentration in the furrow after the inhibition of RhoA by C3 (O'Connell *et al.*, 1999). In addition, myosin-null *Dictyostelium* are able to cleave on adhesive substrates but not in suspension, suggesting ingression in such circumstance may be traction driven (Gerisch and Weber, 2000; Uyeda and Nagasaki, 2004). To reconcile these observations, Wang proposes several alternative mechanisms including cortical sinking mechanism, cortical ripping mechanism, polar relaxation and polar expansion-equatorial compression mechanism and global contraction-equatorial deformation mechanism (Wang, 2005). New experiments need to be designed to address these possibilities.

Ingression of the equatorial cortex appears to be powered by the myosin II motor activity, as inhibition of myosin II contractility by Y-27632 (ROCK inhibitor) and ML-7 (MLCK inhibitor) both slows down furrow ingression (Kosako *et al.*, 2000; Murthy and Wadsworth, 2005; Zhou and Wang, 2008). Treatment with blebbistatin, a myosin

ATPase inhibitor, causes further, complete inhibition of furrow ingression (Straight *et al.*, 2003). However, the exact working location of myosin II needs further clarification, as localized release of blebbistatin near the polar cortex causes abnormality in cytokinesis while the release near the equator causes inhibition of cytokinesis (Guha *et al.*, 2005), suggesting that myosin may play a role throughout the cortex.

The equatorial cortex undergoes not only contraction but also constant structure disassembly during ingression, as suggested decades ago by structural analysis showing that the thickness of the cortex remains constant during ingression despite the decrease in equatorial radius (Schroeder, 1972). Studies using FRAP analysis further suggested that the actin cortical structure is very dynamic during cytokinesis, undergoing constant assembly and disassembly (Pelham and Chang, 2002; Guha *et al.*, 2005; Murthy and Wadsworth, 2005). The actin binding protein cofillin is believed to disassemble actin filaments during cytokinesis (Gunsalus *et al.*, 1995). Recent studies further indicate that myosin II ATPase activity is also required for cortical actin turnover and actin disassembly during furrow ingression (Guha *et al.*, 2005; Murthy and Wadsworth, 2005), as suggested by the decrease of actin turnover rate after blebbistatin treatment.

Mitotic rounding and post-mitotic spreading

During mitosis, animal cells undergo drastic morphological changes, from an interphase spread cell shape to a rounded shape. It is assumed that this morphological transition is important for cell division. Theoretically, a rounded symmetrical cell shape would help create more space along the vertical dimension for mitotic spindle assembly and allow efficient partitioning of the cytoplasm between the two daughter cells. It is

reasonable to speculate that the disassembly of cytoskeletal structures such as stress fibers will create a more favorable environment for microtubules to catch, align, and separate chromosomes, and for the contractile cortex to bisect a cell into two. However, the mechanism of mitotic rounding and post-mitotic spreading is still poorly understood and many questions remain to be answered. For example, what are the driving and regulatory mechanisms, and how important are they in relation to other events in mitosis and cytokinesis? It is possible that the same mechanism may regulate both mitotic rounding and post-mitotic spreading but in opposite directions.

Mitotic rounding involves disassembly of interphase cytoskeletal structures such as focal adhesions and stress fibers, which causes the cell edge to retract and detach from the substrate. A few studies found that some focal adhesion proteins including paxillin and focal adhesion kinase (FAK) are specifically phosphorylated during mitosis (Yamaguchi *et al.*, 1997; Yamakita *et al.*, 1999). The phosphorylation of FAK uncouples signal transduction pathways mediated by integrin, CAS and c-Src, and may maintain FAK in an inactive state until post-mitotic spreading (Yamakita *et al.*, 1999). Phosphorylation of paxillin and degradation of paxillin proteins are also observed in mitosis (Yamaguchi *et al.*, 1997). Rho and Rac GTPase activities may also be regulated, to reduce ruffling activities and stress fiber formation.

It is possible that Cdk1 activity may be responsible for phosphorylating FAK and other cortical proteins to cause cell rounding. The time course of cell rounding appears to correlate with the increase of Cdk1 activity. Careful observations indicated that cells first stop ruffling and show slight retractions at the edge when the nucleus shows signs of chromosome condensation. At this stage, most of the Cdk1 activity is known to

concentrate in the nucleus. However, the rounding process greatly accelerates immediately after nuclear membrane break down, when the Cdk1 activity spreads to the cytoplasm (unpublished). However, it remains to be determined whether Cdk1 is the sole kinase that drives the cytoskeletal reorganization.

It is speculated that myosin II may be the motor that drives the rounding process. However, inhibition of myosin II motor activity does not inhibit cell rounding, though cells do show a slower rate of rounding and incomplete retraction of the cell edge (Guha *et al.*, 2005). Myosin II also appears to help disassemble adhesion structures. In addition, myosin II appears to help coordinate the rounding process with mitosis and maintain an adequate cortical tension, as suggested by the observation that cells continue to shrink during anaphase upon the inhibition of myosin II, while control cells reach maximal rounding in metaphase and start to expand in anaphase (Guha *et al.*, 2005). A recent study also pointed out that myosin II is not the major player in mitotic rounding. Instead, a cross-linking protein moesin appears to be responsible for the reorganization of cortical structure in mitosis (Kunda *et al.*, 2008). It further suggested that cortical structures can provide cues to mitotic spindle assembly. Interesting, it is the stiffness of the cortex, rather than the cell shape, that seems to affect mitotic spindle assembly (Kunda *et al.*, 2008).

Post-mitotic spreading involves reformation of interphase cytoskeletal structure. Cells with inhibited myosin II motor activity are still able to generate large lamellipodium during post-mitotic spreading, suggesting that myosin II is not required (Guha *et al.*, 2005). This finding is consistent with the interphase phenotype of myosin II knock-down cells (Even-Ram *et al.*, 2007). What initiates post-mitotic spreading remains

unclear. Manipulation of Cdk1 activity by drug treatment appears to be enough to induce mitotic rounding and post-mitotic spreading (Potapova *et al.*, 2006). However, further evidence is needed to confirm the role of Cdk1.

An interesting phenomenon in mitotic rounding is the retraction fiber structure left on the substrate by mitotic cells. These retraction fibers have also been observed in some migrating cells and are believed to help rear retraction, although their exact function in cell migration is unclear (Chen, 1981; Lauffenburger and Horwitz, 1996; Kirfel *et al.*, 2003; Wolf *et al.*, 2003). Integrins and some focal adhesion proteins are reported to be present in these retraction fibers (Kirfel *et al.*, 2003). The relationship of the retraction fibers to those in post-mitotic spreading and their function in post-mitotic spreading remain poorly understood.

Chapter II - Myosin II is Required for Cortical Actin Turnover during Cytokinesis

Abstract

The involvement of myosin II in cytokinesis has been demonstrated with microinjection, genetic, and pharmacological approaches, however the exact role of myosin II in cell division remains poorly understood. To address this question, dividing normal rat kidney (NRK) cells were treated with blebbistatin, a potent inhibitor of the non-muscle myosin II ATPase. Blebbistatin caused a strong inhibition of cytokinesis but no detectable effect on the equatorial localization of actin or myosin. However, while these filaments dissociated from the equator in control cells during late cytokinesis, they persisted in blebbistatin-treated cells over an extended period of time. The accumulation of equatorial actin was caused by the inhibition of actin filament turnover, as suggested by a 2-fold increase in recovery halftime after fluorescence photobleaching. Local release of blebbistatin at the equator caused localized accumulation of equatorial actin and inhibition of cytokinesis, consistent with the function of myosin II along the furrow. Treatment of polar region also caused a high frequency of abnormal cytokinesis, suggesting that myosin II may play a second, global role. These observations indicate that myosin II ATPase is not required for the assembly of equatorial cortex during cytokinesis, but is essential for its subsequent turnover and remodeling.

Results and Discussion

Myosin II is partially involved in mitotic cell rounding

As was reported previously, blebbistatin s-(-) at 100 μM caused complete inhibition of cytokinesis (Straight *et al.*, 2003). Furthermore, the s-(+) control isomer had no effect on cytokinesis or actin organization (not shown). Under my experimental conditions there was no detectable effect of blebbistatin on mitosis, and all observed mitotic cells entered anaphase onset without a noticeable delay. Immunofluorescence of microtubules also showed a normal organization (not shown). However, furrow ingression failed within 3-4 minutes of exposure of anaphase cells to blebbistatin, indicating that the drug was quick to enter the cell and to inhibit the myosin II ATPase. In addition, recovery occurred within 15 minutes of the replacement of medium, indicating that the drug dissociated readily from the binding sites. The reversibility allowed applications of the compound both globally and locally (described later), for probing the function of myosin II in various regions.

Morphological effects of globally applied blebbistatin on dividing cells were observed as early as prometaphase, when normal cells underwent striking retraction and rounding, Blebbistatin-treated cells showed persistent, disorganized retractions and ingressions, generating multiple processes and a highly irregular cell shape (Figure 2.1A, Supplemental video 2.1). The irregular morphology was similar to what was found with the Rho inhibitor C3, which inhibits myosin II indirectly through deactivation of the Rho-dependent kinase (O'Connell *et al.*, 1999). However, cells treated with C3 failed to form concentrated band of actin and myosin along the equator as discussed below.

Figure 2.1 Impaired mitotic retraction of NRK cells in the presence of blebbistatin. Blebbistatin was applied to a culture dish for 20 minutes and a field containing mitotic cells was identified for time-lapse recording. A mitotic cell (A, arrowhead) shows a highly irregular shape and several strands of cytoplasm that failed to retract (A, arrows). However, chromosomal separation appears unaffected for all the mitotic cells in this field (see Supplemental Video 2.1). Bar, 40 μm. Quantitative analysis, by measuring the percentage decrease in cell area relative to the corresponding cell area at prophase for 5 control cells and 6 blebbistatin treated cells, indicates that blebbistatin induces a delay in rounding (B; PR, prophase; PM, prometaphase; M, metaphase, A, anaphase). Error bars indicate S.E.M. Retraction of treated cells continues well after anaphase onset and reaches a similar average extent as do control cells at a later time point.

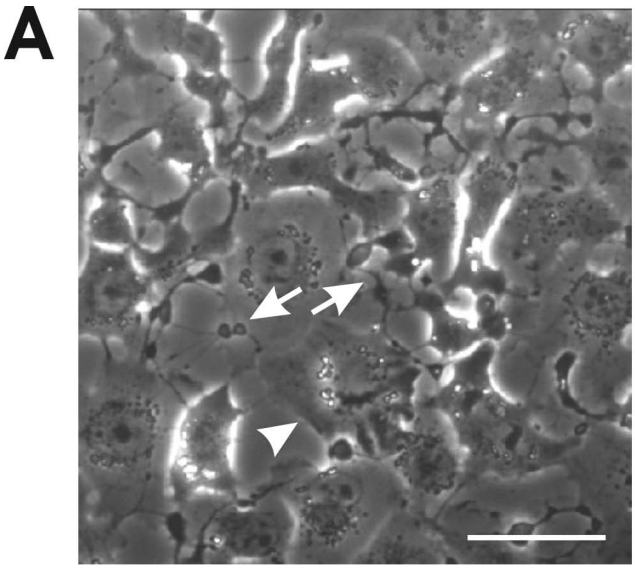
A

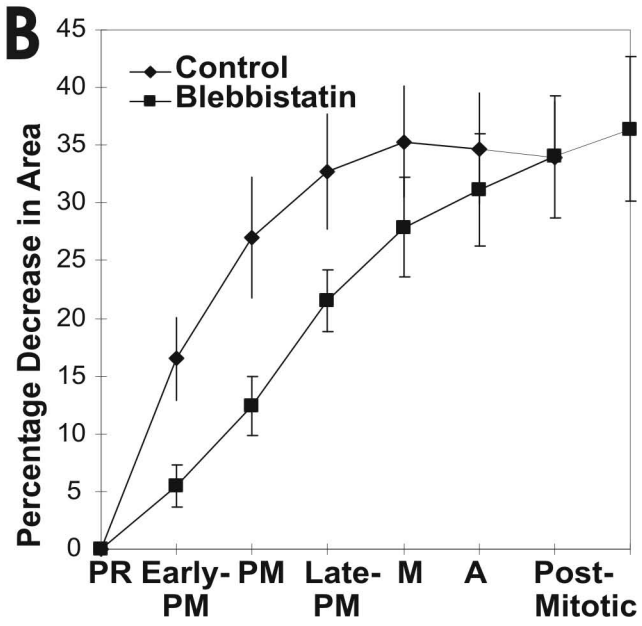
B
Control
Blebbistatin
Percentage Decrease in Area
0
5
10
15
20
25
30
35
40
45
PR
Early-PM
PM
Late-PM
M
A
Post-Mitotic

Quantitative analysis of the spreading area indicated a decrease in the rate of mitotic retraction that lasted well beyond anaphase onset, while control cells reached maximal rounding by metaphase (Figure 2.1B). However, most blebbistatin-treated cells eventually reached a similar extent of rounding as did control cells (Figure 2.1B), suggesting that myosin II motor activity is involved in mitotic rounding but does not exclusively account for the activity. Unlike cells treated with butadione monoxime (Cramer and Mitchison, 1995), blebbistatin-treated cells showed no apparent inhibition of the postmitotic respreading process (Supplemental video 2.1).

Myosin II ATPase activity is not required for equatorial actin and myosin II assembly during early cytokinesis

Cells treated with 100 μM blebbistatin were first stained for actin filaments and myosin II. Equatorial actin assembly during early anaphase appeared uninhibited by blebbistatin (Figure 2.2A), as indicated by the organization of actin filaments and the normal extent of actin localization along the equator of treated and control cells (Figure 2.2A-C). Myosin II showed a similar equatorial concentration in the presence of blebbistatin as in control cells (Figure 2.2A and B).

The above observations suggest that myosin does not rely on its own motor activity to drive itself to the equatorial region, consistent with the previous observation of normal equatorial organization of myosin with defective heads (Yumura and Uyeda, 1997; Zang and Spudich, 1998). They similarly argue against a myosin II-driven equatorial contraction mechanism that causes the cortical actin network to collapse and concentrate into the equator (White and Borisy, 1983). Further, the results suggest that the inhibition

Figure 2.2 Effects of blebbistatin on the assembly and disassembly of equatorial actin and myosin. A dish was treated with blebbistatin for 20 minutes before fixation, and images of phalloidin or myosin IIa immuno-staining were collected from cells at various stages of division. Myosin IIa and actin filaments show a similar increase in equatorial concentration during early anaphase in control (B) and blebbistatin treated cells (A). However, after the completion of mitosis, both actin and myosin II disappear from the cleavage site in control cells (B; right column; the concentration of actin between the daughter cells is due to the formation of cell-cell junctions), but persist in the equatorial region of blebbistatin treated cells (A; right column). Bar, 40 μm. Integration of the intensity of phalloidin staining in the equatorial region versus the whole cell indicates that equatorial actin filaments persist in blebbistatin treated cells (C; left bars), whereas control cells show a striking decrease shortly after anaphase onset (C; right bars). The graph was generated from the measurements of 4-8 control or treated cells at each stage. Error bars indicate S.E.M. The persistent band of equatorial actin defines a region that resists anaphase retraction in blebbistatin-treated cells, causing some cells to form a bulge along the equator (D). Bar, 40 μm.

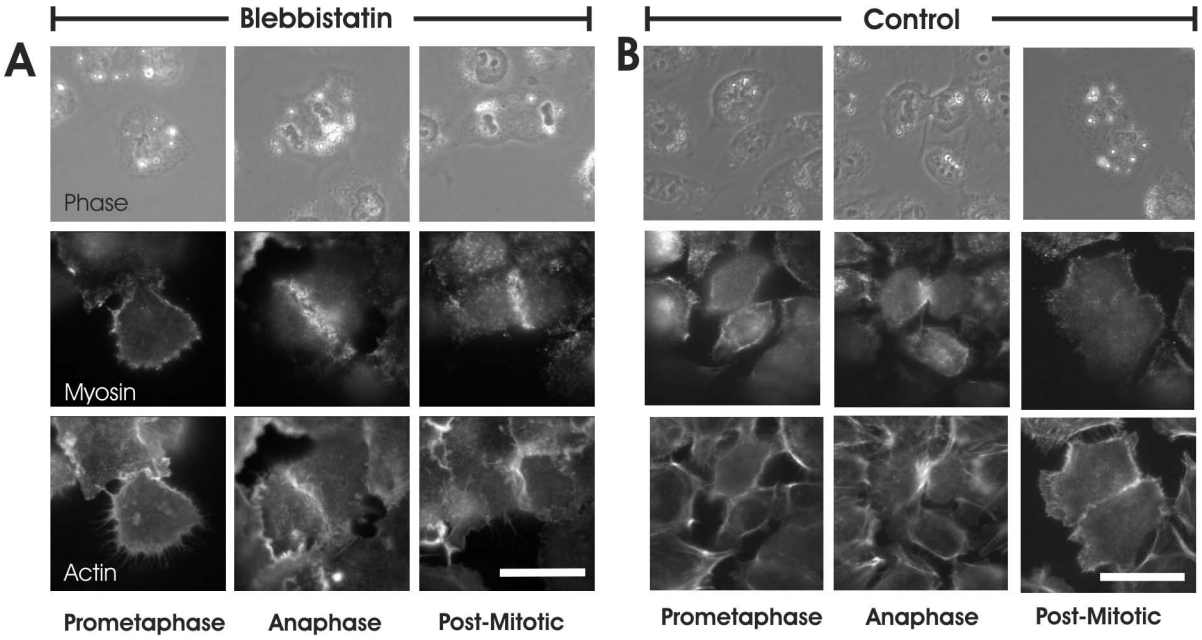
A
Blebbistatin
Phase
Myosin
Actin
Prometaphase
Anaphase
Post-Mitotic
B
Control
Prometaphase
Anaphase
Post-Mitotic

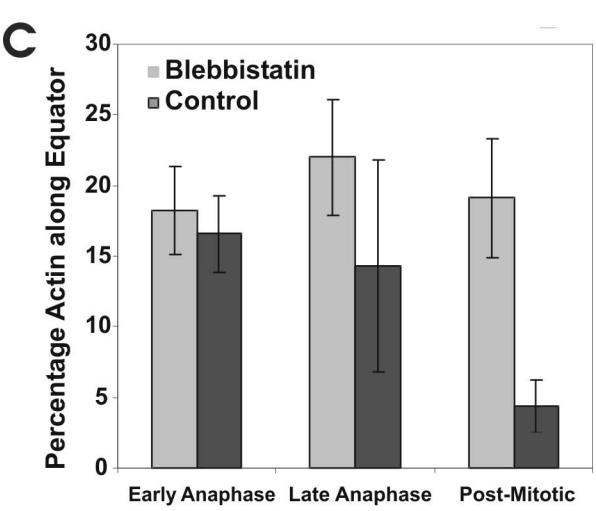
C
Percentage Actin along Equator
30
25
20
15
10
5
0
Blebbistatin
Control
Early Anaphase
Late Anaphase
Post-Mitotic

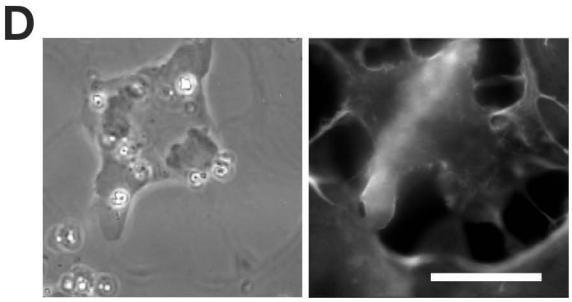
D

of cytokinesis by blebbistatin is not caused by a defect in equatorial cortical assembly, but defects in subsequent steps.

Myosin II ATPase activity is required for actin and myosin disassembly during late stages of cell division

The dissociation of actin and myosin II from the equatorial region during and after late anaphase was examined. In blebbistatin-treated cells, both actin and myosin II persisted along the equator long after (>30 minutes) the separation of chromosomes (Figure 2.2A and C). In contrast, control cells showed a striking decrease in the percentage of actin filaments along the equator following anaphase onset (Figure 2.2B and C). These results indicate that myosin II ATPase activity is required for the post-mitotic dissociation of equatorial actin and myosin II filaments. The accumulating filaments may inhibit not only cortical ingression but also retraction along the equator, causing the equatorial region to form a bulge as seen in some treated cells (Figure 2.2D).

To determine if the inhibition of actin dissociation was due to a decrease in the dynamics of cortical actin network, FRAP (fluorescence recovery after photobleaching) analysis was performed on cells microinjected with rhodamine-labeled actin. Fluorescence recovery for both experimental and control cells at early anaphase showed a halftime of about 12-15 sec (Figure 2.3), indicating that equatorial cortex at this stage is highly dynamic and that the dynamics is independent of myosin motor activities. However, at later stages when the equatorial band became well organized, blebbistatin-treated cells showed a two-fold increase in recovery halftime to 25-30 sec, while the

Figure 2.3 FRAP analysis of actin dynamics in control (right bars) and blebbistatin treated cells (left bars). Cells were injected with rhodamine actin during prometaphase, treated with blebbistatin after 10-15 minutes of recovery, and bleached in the equatorial region within 1-2 minutes ("Early Anaphase") or >5 minutes ("Late Anaphase-Telophase") of anaphase onset. The halftime of recovery shows no significant difference during early anaphase, but a 2-fold increase in blebbistatin treated cells as compared to control cells during a later stage. Moreover, similar increases in halftime are observed both along and out of the equatorial region. Each halftime represents the average from 4-6 measurements. Errors bars indicate S.E.M.

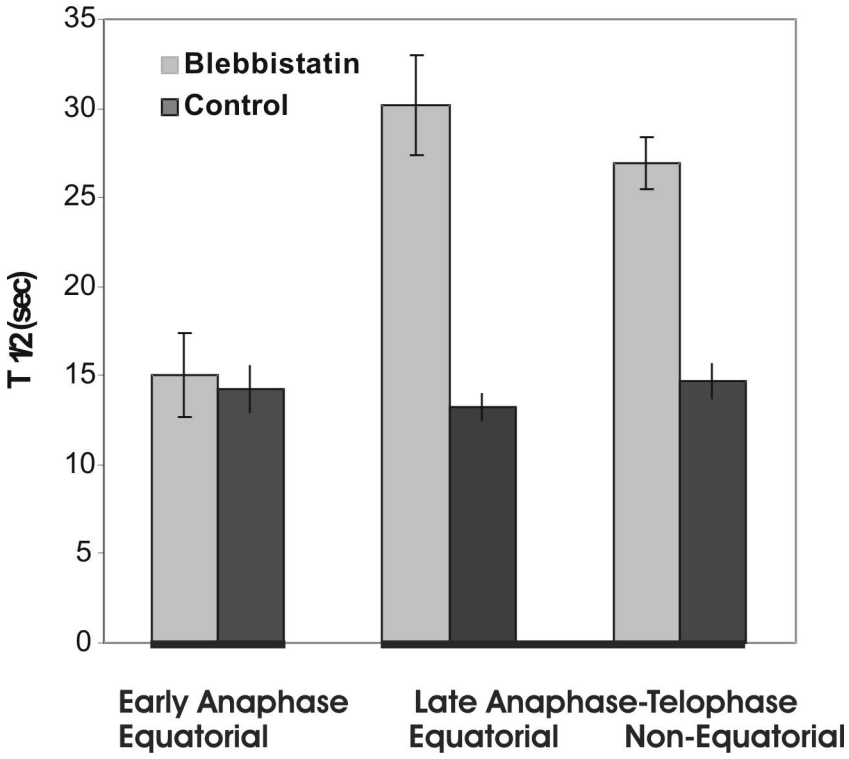
35
30
25
20
15
10
5
0
T 1/2 (sec)
Blebbistatin
Control
Early Anaphase
Equatorial
Late Anaphase-Telophase
Equatorial
Non-Equatorial

halftime for control cells remained unchanged throughout cytokinesis (Figure 2.3). Similar differences in halftime between control and treated cells were observed outside the equator (Figure 2.3). Together, these observations suggest that mitotic exit has a global effect in stabilizing the actin cortex, and that myosin II motor activities are required for maintaining the dynamics. It is worth noting that the amount of myosin in the furrow accounts for only about 10% of the total cellular myosin in *Dictyostelium* (Robinson *et al.*, 2002). Although the concentration of myosin II is higher along the equator than other cortical regions, the ratio of myosin II to actin filaments is likely to be similar throughout the cortex, which explains the similar rate of actin turnover in control cells.

The delayed recovery, together with the accumulation of equatorial actin filaments, indicates that myosin II motor activity is crucial for the turnover of actin filaments in the equatorial region. The process could involve either “ripping” of actin filaments from the membrane by the contractile forces, or activation of an actin-severing or depolymerization mechanism. Such cortical disassembly process has been implicated in earlier ultrastructural analysis (Schroeder, 1972), and is likely responsible for removing the accumulating cortical materials in order for the ingression to continue.

Myosin II functions both along and outside the equatorial region during cytokinesis

It was reported that local application of cytochalasin D at the equator not only failed to inhibit cytokinesis, but appeared to facilitate the furrowing process (O'Connell *et al.*, 2001). In contrast, application of cytochalasin D near the spindle poles inhibited cytokinesis. This raised the provocative possibility that crucial actin-myosin interactions

for cytokinesis may occur outside the equatorial region. To address this question, blebbistatin was applied to a small (10-15 μm diameter) region at the equator, by using a microneedle to release the drug close to the cell cortex while simultaneously removing the medium with a nearby suction needle (Figure 2.4A; (O'Connell *et al.*, 2001)). The treatment caused inhibition of ingression (~60% of cells), as did global applications (Figure 2.4B and Video 2.2). Phalloidin staining of these cells showed a strong accumulation of actin filaments on the side facing the needle (Figure 2.4C), while local treatment with DMSO-containing carrier solution had no effect on cytokinesis (not shown; (O'Connell *et al.*, 2001)). Although the inhibitory effect of blebbistatin is opposite that of cytochalasins, it may be explained if myosin II, like cytochalasins, promotes the disassembly of actin filaments during the force-generating interactions. The effect of blebbistatin is similar to that of jasplakinolide, which inhibits ingression by stabilizing the equatorial actin network (O'Connell *et al.*, 2001).

To investigate if myosin II also functions outside the equator, blebbistatin was applied near the polar region. The treatment caused only a small percentage of cells to fail cytokinesis (<10%). However, a large percentage of cells (~60%) showed various degrees of abnormality (Figure 2.4A and B and Supplemental video 2.3), including asymmetric ingression, misplaced cleavage furrows (Supplemental video 2.3), and top-to-bottom divisions with little lateral ingression, effects not observed with equatorial application even at suboptimal doses. These results suggest that cytokinesis involves not only contractions and cortical assembly/disassembly along the equator, but possibly a global balance among contractile forces, cortical rigidity, and structural integrity.

Figure 2.4 Effects of localized treatment with blebbistatin. A cell treated at the equator shows inhibition of cytokinesis on the side facing the needle (A; upper row). The other side shows normal cytokinesis as indicated by the arrows. A cell treated near the pole shows misplaced ingression (A; lower row, upper arrows), located far away from the equator and near separated chromosomes. Numbers indicate time in seconds. Analysis of 15 cells treated along the furrow, and 25 cells near the pole, shows a high percentage of cleavage failure with equatorial treatment, and a high percentage of abnormal cleavage (top-down division and mis-placed furrow) with polar treatment (B). A cell treated at equator (C, left panel, arrow) shows strong accumulation of actin filaments along the side facing the needle. Cells treated near the pole (C, right panel, arrow) show an equatorial actin organization similar to that in control cells. Bar, 40 μm.

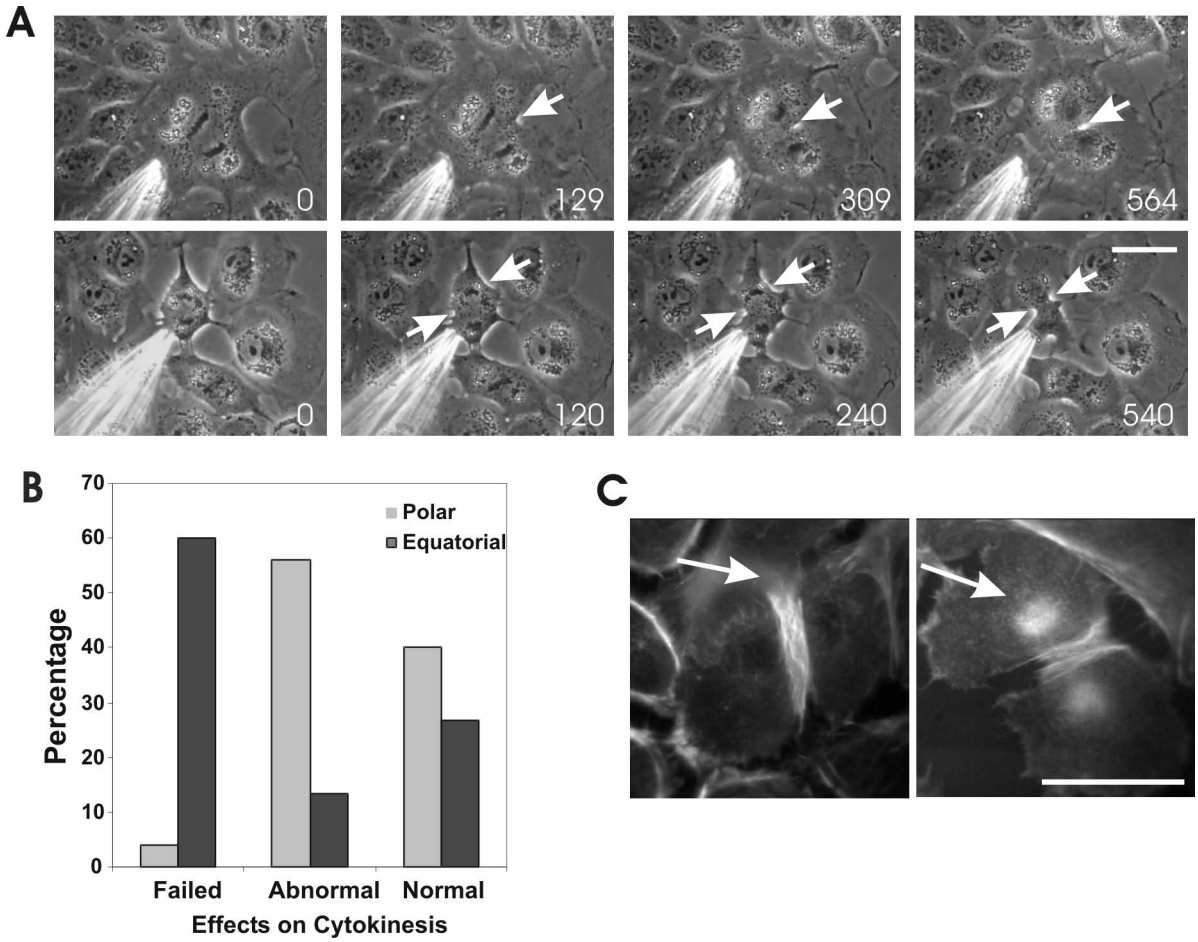
A
0
129
309
564
0
120
240
540
B
70
60
50
40
30
20
10
0
Percentage
Polar
Equatorial
Failed
Abnormal
Normal
Effects on Cytokinesis
C

Materials and Methods

Cell Culture, Drug Treatment, and Microscopy

NRK epithelial cells (NRK52E; American Type Culture Collection) were cultured as described previously (McKenna and Wang, 1989). They were subcultured onto cover glass chamber dishes 12-24 hours before the experiment. Blebbistatin (s-(-) isomer; Toronto Research, Toronto, Canada), or the s-(+) control (EMD Biosciences, San Diego, CA), was dissolved with 90% DMSO to make a stock solution of 100 mM, which was diluted 1:1000 with supplemented F-12K medium to obtain a working concentration of 100 μM. Following replacement of the medium, the culture chamber was incubated for a minimum of 20 min prior to recording or fixation. Fixation and fluorescent staining were performed as described previously (O'Connell *et al.*, 1999). Antibodies against myosin IIa were obtained from Covance Research.

Since blebbistatin is known to be light sensitive (Kolega, 2004), microscope lamp intensity was maintained at a minimum and red cellophane filters (Edmund Scientific, Barrington, NJ) were used during the observation of live cells,. Images were acquired with a 40X, NA 0.75 Plan-Neofluar phase or a 100X, NA 1.30 Plan-Neofluar phase lens (Carl Zeiss, Thornwood, NY) and a cooled CCD camera (NTE-CCD-EBFT; Roper Scientific, Trenton, NJ), and processed with customized digital imaging software for background subtraction. Integrated fluorescence intensity along the equator (defined as the region with a concave lateral border during anaphase and telophase) and within the whole cell was also obtained using custom software. Mitotic cell rounding was calculated by dividing the spread area, measured as the number of pixels within a manually drawn cell boundary, with the area of the same cell during prophase.

Micromanipulation and Local Drug Application

Stock solution of blebbistatin was mixed with 25 mg/ml red fluorescent dextran (Molecular Probes, Eugene, OR) in warm, supplemented F-12K medium to obtain a working concentration of 850 μM blebbistatin, 1 mg/ml dextran, and 1% DMSO. The solution was clarified at 25,000 RPM for 20 min in a Type 42.2 Ti rotor (Beckman Coulter, Fullerton, CA). Localization of blebbistatin was achieved by using a release needle paired with a suction needle (O'Connell *et al.*, 2001); the latter was prepared by breaking the tip of a microneedle and fire polishing with a microforge (Narishige USA, Sea Cliff, NY). The needles were mounted on a custom made double micromanipulator and the flow regulated with a combination of regulated compressed air and vacuum. NRK cells were rinsed with filtered F-12K medium immediately before the experiment, and the culture layered with mineral oil (embryo tested; Sigma, St. Louis, MO) following drug application to prevent evaporation. Alexa-546 phalloidin was prepared and microinjected as described previously (Wang, 1992). Images of injected cells were acquired using spinning-disk confocal optics (Solemere Technology, Salt Lake City, UT), with a diode pumped solid state laser at 532 nm.

FRAP Analysis

Rhodamine labeled muscle actin (Cytoskeleton) was microinjected at a concentration of 0.8 mg/ml, following clarification in an ultracentrifuge. Fluorescence was bleached with the 514 nm line from an Argon laser, at a power of 300 mW and duration of 50 ms. Images during fluorescence recovery were captured every 10 sec with spinning-disk

confocal optics. A 525 nm dichroic mirror (525DRLP; Omega Optical, Brattleboro, VT) was placed in the optical path, to allow simultaneous bleaching with the 514 nm beam and imaging with the 532 nm laser. Fluorescence intensity was measured with custom software and analyzed with Excel (Microsoft). Photobleaching of control cells had no effect on division.

Conclusions

In summary, the present results suggest that equatorial myosin II serves a dual role during cytokinesis; to generate the forces and to disassemble the cortex to allow ingression. However, motor activity of myosin II is not necessary for the assembly of the equatorial band of myosin and actin filaments.

Supplemental Materials

Supplemental Video 2.1. The field as shown in Fig. 2.1A recorded over 51 minutes. Circles in the beginning indicate three dividing cells. Even though cytokinesis fails, these cells show striking shape changes throughout the period of division. Both mitosis and post-mitotic spreading appear to take place normally.

Supplemental Video 2.2. The same sequence as in the upper row of Fig. 2.4A, showing the inhibition of ingression when blebbistatin is applied near the equator.

Supplemental Video 2.3. The same sequence as in the lower row of Fig. 2.4A, showing the misplacement of ingression when blebbistatin is applied near the pole.

Chapter III - Distinct Pathways for the Early Recruitment of Myosin II and Actin to the Cytokinetic Furrow

Abstract

Equatorial organization of myosin II and actin has been recognized as a universal event in cytokinesis of animal cells. Current models for the formation of equatorial cortex favor either directional cortical transport toward the equator, or localized de novo assembly. However, this process has never been analyzed directly in dividing mammalian cells at a high resolution. I applied total internal reflection fluorescence microscope (TIRF-M), coupled with spatial temporal image correlation spectroscopy (STICS) and a new imaging approach termed temporal differential microscopy (TDM), to image the dynamics of myosin II and actin during the assembly of equatorial cortex. The results indicated distinct and at least partially independent mechanisms for the early equatorial recruitment of myosin and actin filaments. Cortical myosin showed no detectable directional flow during early cytokinesis. In addition to equatorial assembly, localized inhibition of disassembly contributed to the formation of the equatorial myosin band. In contrast to myosin, actin filaments underwent a striking flux toward the equator. Myosin motor activity was required for the actin flux, but not for actin concentration in the furrow, suggesting that there was a flux-independent, de novo mechanism for actin recruitment along the equator. The present results indicate that cytokinesis involves signals that regulate both assembly and disassembly activities, and argue against mechanisms that are coupled to global cortical movements.

Introduction

Recruitment of myosin II (referred as myosin later) and actin along the equatorial cortex represents a universal event in cytokinesis. While the function of a narrowly defined "contractile ring" is still under debate (Wang, 2005), it is generally agreed that the organization of actin and myosin filaments along the equator is related to equatorial contractility and cortical ingression. There are two prevailing hypotheses on how myosin and actin are recruited to the equatorial cortex. The cortical flow hypothesis proposes that myosin and actin from the polar cortex flow actively or passively into the equatorial cortex, as a consequence of either directed transport or differential cortical contractions (White and Borisy, 1983; Bray and White, 1988). The structural synthesis hypothesis argues that direct recruitment of molecules or small polymeric building blocks from the cytoplasm is responsible for the formation of the acto-myosin equatorial band (Pelham and Chang, 2001; Wu *et al.*, 2006).

There are experimental evidence for the involvement of both cortical flow and direct structural synthesis in cytokinesis. The former was supported primarily by imaging membrane-bound beads (Wang *et al.*, 1994), fluorescently labeled actin (Cao and Wang, 1990b), or myosin (DeBiasio *et al.*, 1996), in systems from live mammalian cells to *Dictyostelium*. In addition, several theoretical models predicted a concerted flow of cortical actin and myosin into the equator (White and Borisy, 1983; He and Dembo, 1997), as a consequence of global force balance over the cortex. Direct structural synthesis was supported by the appearance and/or growth of punctate acto-myosin structures in dividing frog embryos (Noguchi and Mabuchi, 2001), and yeast (Wu *et al.*, 2006), and by the dependence of cytokinesis on genes that regulate de novo structural

assembly (Gunsalus *et al.*, 1995; Pelham and Chang, 2001; Severson *et al.*, 2002). Although cortical flow and structural synthesis hypotheses are not mutually exclusive, their contributions to the recruitment of equatorial actin and myosin remain unclear. As several hypothetical mechanisms of cytokinesis make strong predictions about how equatorial structures are formed (Burgess and Chang, 2005), detailed analyses of cortical dynamics during early cytokinesis are likely to provide useful new insights.

The limitation to the current knowledge is in part due to the lack of high-resolution images that depict the assembly of equatorial cortex immediately before and during cytokinesis. Because of the strong signals from the cytoplasm, it has been very difficult to observe directly the assembly process in live cells using conventional epi-fluorescence optics. With its very short depth of field (<200 nm) and dramatically reduced background, the total internal reflection fluorescence microscopy (TIRF-M) is uniquely suitable for providing high-resolution images of structural dynamics on the cell cortex (Axelrod, 2001). In this study, I have combined TIRF-M with spatial temporal image correlation spectroscopy (STICS) (Hebert *et al.*, 2005), an approach similar to fluorescence speckle microscopy for precise tracking of the movement of structural inhomogeneities, and temporal differential microscopy (TDM), a novel image analysis method that measures the local kinetics of structural assembly or disassembly. My observations lead to the conclusion that actin and myosin follow distinct pathways to the equatorial cortex. Cortical flow is limited to actin, and is not solely responsible for its equatorial concentration, while myosin is recruited directly from the cytoplasm. In addition, the formation of equatorial myosin band involves the regulation of both assembly and disassembly activities.

Materials and Methods

Cell Culture and Transfection

A subclone of Normal Rat Kidney cells (NRK-52E; American Type Culture Collection, Rockville, MD) was grown on glass coverslips in Kaighan's modified F12 medium (Sigma, St. Louis, MO) supplemented with 10% fetal calf serum (JRH Biosciences, Kansas City, MO), 1 mM L-glutamine, 50 μg/mL streptomycin and 50 U/mL penicillin (Gibco, Carlsbad, CA). Cells were maintained at 37^{o}C in a humidified atmosphere containing 5% CO_2. EGFP-nonmuscle myosin heavy chain IIA and IIB, EGFP-actin, mCherry-actin plasmids were kindly provided by Dr. Robert S. Adelstein (NIH/NHLBI) and Dr. Michael Davidson (Florida State University). Transient transfection of NRK epithelial cells was performed by nucleofection using the Amaxa nucleofector and kit R (Amaxa, Gaithersburg, MD), following manufacturer's protocol. After transfection, cells were plated on glass coverslips and cultured overnight before imaging.

Drug Treatment and Microinjection

The drug concentrations of Y-27632 (Calbiochem, San Diego, CA), (-)-blebbistatin (Toronto Research, Toronto, Canada), (+)-blebbistatin (Calbiochem, San Diego, CA), ML-7 (Calbiochem, San Diego, CA), latrunculin B (Calbiochem, San Diego, CA) were 40 μM, 100 μM, 100 μM, 50 μM, 10-20 μM respectively. For drug experiments, NRK cells at prometaphase were treated for at least 10 minutes before anaphase onset and the drug was maintained during the following period of imaging. C3 transferase (Calbiochem, San Diego, CA) was microinjected at a concentration of 0.5 mg/ml with

fluorescein dextran as a marker (Molecular Probes, Eugene, OR). Injection of fluorescein dextran alone had no effect on mitosis or cytokinesis.

Immunofluorescence

For myosin II staining, cells were fixed in 1% formaldehyde, 0.1% glutaraldehyde, and 0.3% Triton X-100 for 1 minute, followed by postfixation in 0.5% glutaraldehyde for 10 minutes. Myosin IIA was immunostained with anti-nonmuscle myosin IIA polyclonal antibodies (Covance Research, Princeton, NJ) at a dilution of 1:100. To stain for actin filaments, cells were fixed in 4% formaldehyde and 0.2% Triton X-100 for 10 minutes and incubated with Alexa-488-phalloidin or Alexa-546-phalloidin following manufacturer's protocol (Molecular Probes).

Microscopy and Data Collection

Images were collected with either a Zeiss Axiovert-10 or Axiovert-200M inverted microscope (Thornwood, NY), equipped with a 100x, N.A. 1.30 Phase Plan-Neofluar objective lens for conventional epi-fluorescence optics, and a 100x, N.A. 1.45 αPlan-Fluar objective lens for TIRF-M. Light for TIRF-M was generated by a Lexel Model 94, 2W argon ion laser operating at 10 mW, 488 nm for GFP proteins, or a 2.5 mW 543 nm HeNe laser for mCherry-actin (Model LHGR-0200, Research Electro Optics, Boulder, CO). The laser beam was expanded with a beam expander, and directed into the microscope using a focusing lens and several steering mirrors, adjusted such that the beam exits the objective lens as a parallel beam at an angle exceeding the critical angle for total internal reflection. Fluorescence images were collected with a cooled CCD

camera (Model NTE/CCD-512-EBFT, Princeton Instrument, Trenton, NJ, or Model DV-887-DCS-BV, Andor Technology, Belfast, UK), with 0.5 or 1 sec exposure, and subtracted with a dark-count image. Except for linear adjustments across the entire image to optimize the display, the images were unaltered. Data acquisition and analyses were performed with a combination of custom software, ImageJ (NIH) and Excel (Microsoft).

Image Analysis

Standard image analysis procedures, including kymograph analysis and intensity integration, were performed with a combination of custom software, ImageJ (NIH) and Excel (Microsoft). STICS was implemented as custom software, using a similar cross-correlation approach as described previously (Hebert *et al.*, 2005; Ji and Danuser, 2005). Each set of displacement vectors was generated by averaging displacements detected in a set of 5 consecutive frames taken over ~12 seconds. The detection window for movements was set at 1.3x1.3 μm^2 as the default and adjusted adaptively as described by Ji and Danuser (2005). TDM was also implemented as custom software. It involved pixelwise computation of the intensity differential, $(I_{t+\Delta t} - I_t)/(I_{t+\Delta t} + I_t)/\Delta t/2$ where I_t is the average intensity around the pixel at time t and $\Delta t \approx$ 4-7 seconds. This quantity equals approximately the local rate of percentage change in intensity. To control the noise some images were filtered with a median filter before the computation. For visualization, the resulting positive or negative values were scaled linearly and rendered in pseudo-color.

Results

TIRF-M provides high-resolution images of cortical structure of myosin and actin in cytokinetic cells

To visualize myosin and actin in live cells, I expressed GFP-tagged nonmuscle myosin II heavy chain (referred as GFP-myosin later), or GFP- or mCherry-tagged actin in normal rat kidney (NRK) epithelial cells, which remained relatively flat during mitosis and were ideal for microscopy. These tagged proteins served as reliable probes for endogenous structures (Figure 3.1 and Figure 3.2A). Compared to conventional epi-fluorescence optics, TIRF-M provided a much higher resolution of cortical structures in mitotic cells (Figure 3.2A). GFP-myosin was found in dot-like structures with an average area of 0.2 μm^2 (or an equivalent diameter of 0.5 μm, which may be partially diffraction-limited), throughout the cortex of mitotic cells. From the lack of abrupt bleaching, these dots likely represent myosin minifilaments or small clusters of minifilaments as described previously (Verkhovsky and Borisy, 1993; Maupin *et al.*, 1994), rather than single molecules. Cortical actin on dividing cells consisted of dots, patches, short fibers, and diffuse structures (Figure 3.2A).

Soon after anaphase onset, prominent myosin dots and actin filament structures appeared on the equatorial cortex, forming a prominent band before the initiation of ingression (Figure 3.2A). GFP-myosin band appeared along the equator slightly earlier than GFP-actin, becoming detectable at about 60 seconds and 100 seconds after chromosome segregation respectively (Figure 3.2B), suggesting that they may follow different pathways.

Figure 3.1 GFP-nonmuscle myosin IIA heavy chain and GFP-actin as functional probes in interphase NRK cells. Expressed proteins become incorporated into stress fibers and focal adhesions (A, arrows), as imaged by TIRF-M. Images of GFP-actin and Alexa-546-phalloidin staining show extensive colocalization, suggesting GFP-actin is incorporated into most if not all actin filament structures (B, orange arrows indicate equator). In addition, transfected cells grow and divide normally.

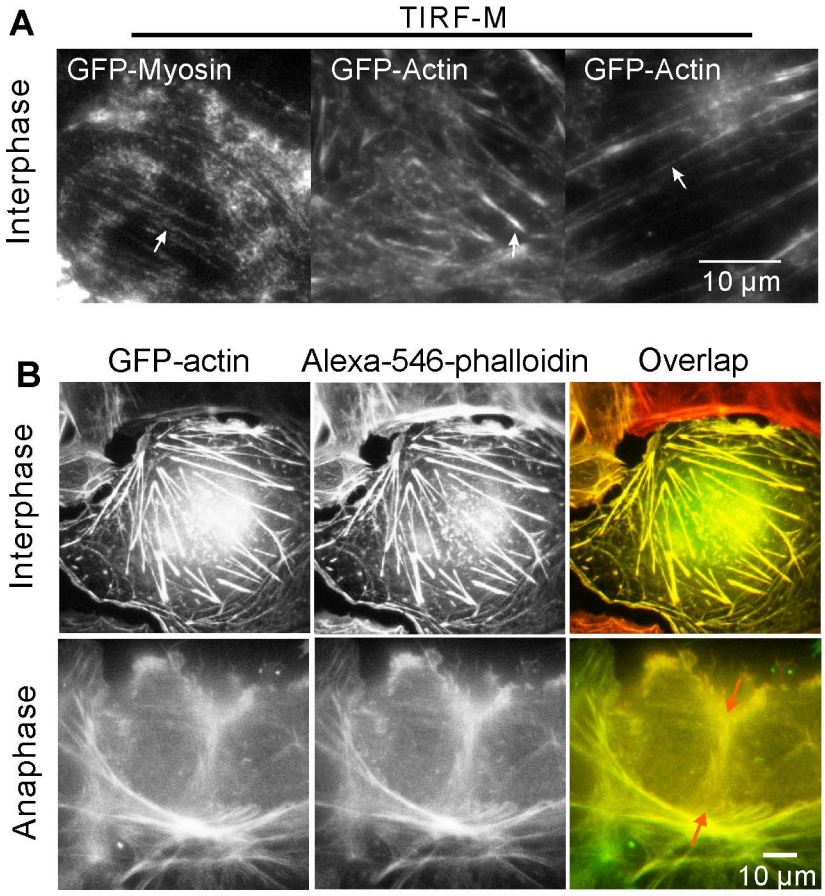
A
TIRF-M
Interphase
GFP-Myosin
GFP-Actin
GFP-Actin
10 µm
B
GFP-actin
Alexa-546-phalloidin
Overlap
Interphase
Anaphase
10 µm

Figure 3.2 High-resolution imaging of cortical myosin and actin structure in mitotic cells with TIRF-M. GFP-nonmuscle myosin IIA heavy chain or GFP-actin accumulates along the equator, which is detected as a fuzzy band using conventional epi-fluorescence optics (A, left panels, arrows indicate the equator). TIRF-M provides a much higher resolution than epi-fluorescence, revealing fine cortical structures of myosin and actin (A, middle and right panels). Staining of endogenous myosin and actin (A, right panels) shows similar structures as those seen with GFP-myosin and GFP-actin in live cells (A, middle panels). GFP-myosin band appears in the equator slightly earlier than GFP-actin (B). Time (sec) is measured from chromosome segregation to the first detection of GFP-myosin or GFP-actin concentration along the equator (n=10 each for actin and myosin; error bars indicate the standard deviation)

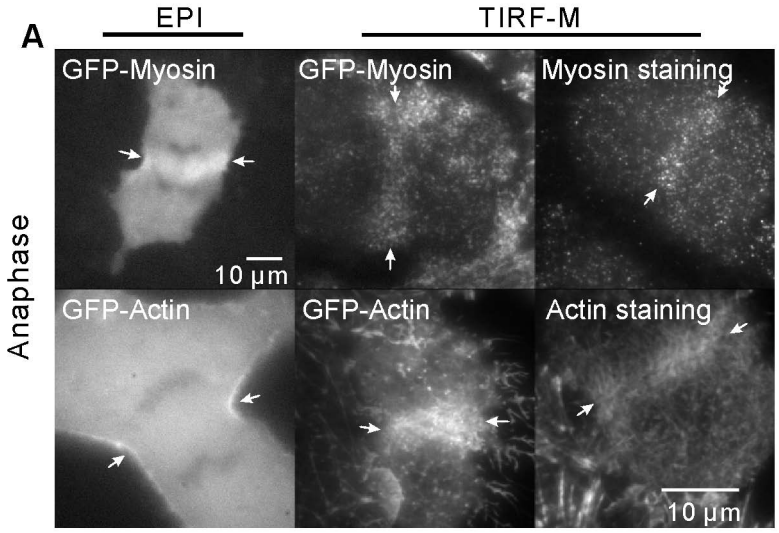
A
EPI
TIRF-M
GFP-Myosin
GFP-Myosin
Myosin staining
10 µm
Anaphase
GFP-Actin
GFP-Actin
Actin staining
10 µm

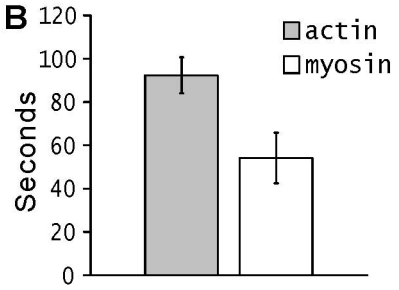
B
120
100
80
60
40
20
0
Seconds
actin
myosin

Myosin shows no detectable cortical flow in early cytokinesis

To determine if the assembly process of equatorial myosin involves cortical flow, as has been suggested previously (White and Borisy, 1983), I collected time-lapse TIRF-M movies of dividing cells expressing GFP-myosin. Direct observations of cortical myosin in more than 20 cells provided no indication of directional movement toward the equator during early equatorial assembly (Figure 3.3A, Supplemental Video 3.1). Moreover, kymograph analysis showed only horizontal tracks indicating that there was no long-range movement of myosin throughout the cortex along any directions (Figure 3.3B). Consistent results were obtained with STICS, which tracked the movement of features within 1.3 x 1.3 μm^2 regions (Figure 3.3C). The increase in equatorial myosin concentration appeared to involve a combination of an increase in the intensity of pre-existing myosin structures, and de novo appearance of new myosin dots along the equator (Figure 3.3A and B d, e, boxed areas), which together lead to a 45±12% increase in average intensity along the equator during a 30 second interval in early cytokinesis. The flanking regions showed a concomitant intensity decrease of 14±6% (Figure 3.3D), suggesting changes in the relative association and dissociation kinetics between the equatorial region and the rest of the cortex.

Cortical myosin assembly/association appears in dynamic domains throughout the cortex

TIRF-M time-lapse recording of cortical myosin revealed an intriguing phenomenon. Contrary to the common notion that myosin builds up directly and locally along the equator, I observed domains over the entire cell cortex where myosin intensity showed

Figure 3.3 Lack of detectable cortical flow of myosin during early cytokinesis. Selected frames from a TIRF-M time-lapse sequence of cells expressing GFP-myosin show the rapid recruitment of myosin onto the equatorial cortex over a period of 30 seconds (A, upper panels; bottom panels are the enlarged view of the equatorial region). Kymograph analysis of cortical myosin in different regions and along different directions (B, white rectangular boxes, left panels) shows no directed movement of cortical myosin dots during early assembly of the equatorial cortex (B, right panels). However, myosin dots in the equatorial region were more stable, as indicated by longer horizontal lines in kymographs (B, right panels). In addition, some myosin dots in the equatorial region gain intensity, while other dots appear to form de novo (B, boxes in kymographs of d, e). Analysis with STICS shows no significant coordinated movements of structures within detection windows of 1.3 x 1.3 μm^2 throughout the cortex (C; yellow arrows indicate displacement velocity, cutoff velocity = 6 nm/sec). The scale bar also represents a speed of 0.22 μm/sec in STICS (C). Analysis of integrated fluorescence intensities over a period of 30 seconds during early cytokinesis indicates an increase of average intensity by 45% along the equator, and a decrease by 14% in the flanking region (D; n=5, error bars indicate the standard deviation). Supplement Video 3.1 shows the corresponding movie.

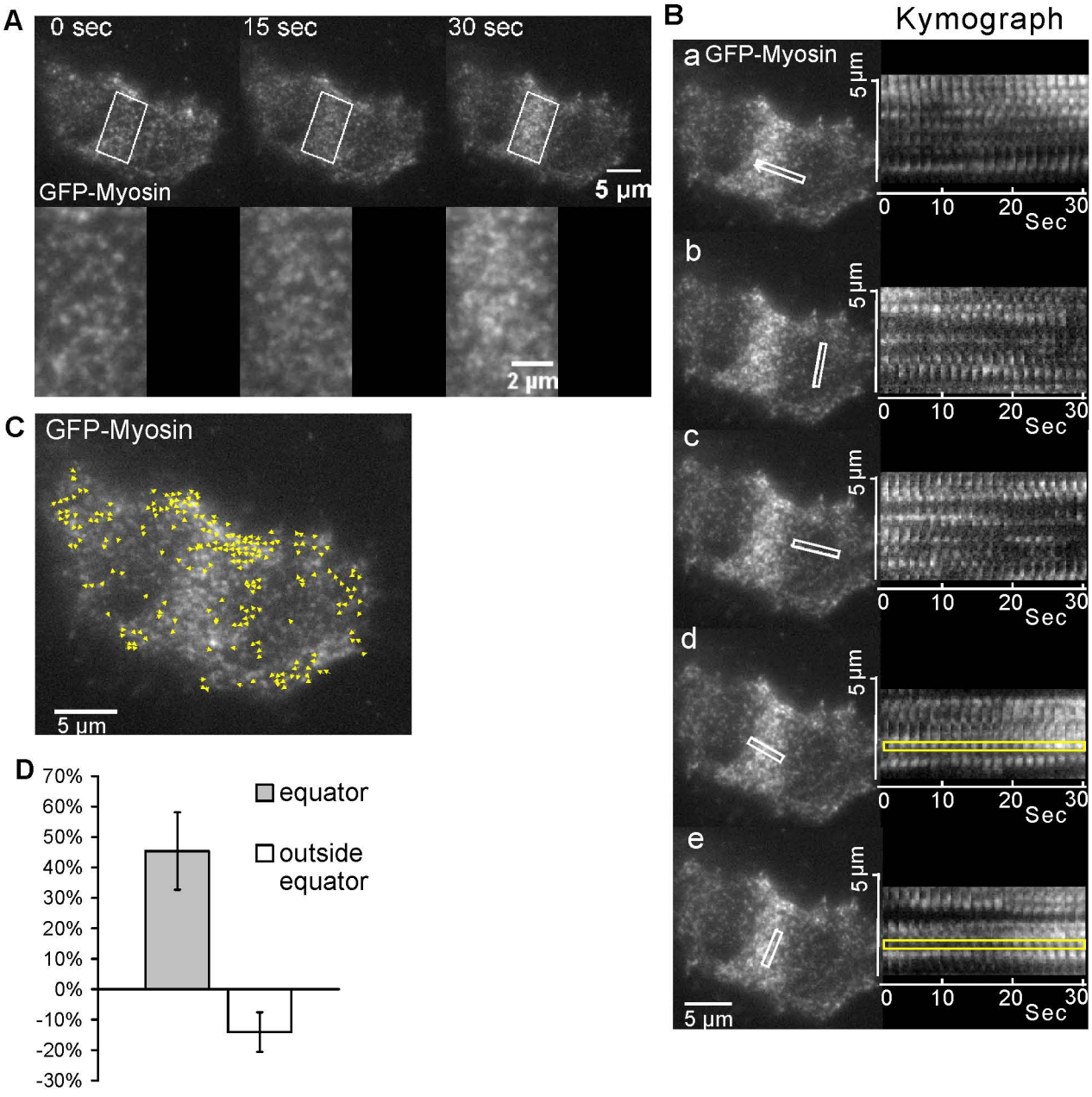
A
0 sec
15 sec
30 sec
GFP-Myosin
5 µm
2 µm
B
Kymograph
a GFP-Myosin
b
c
d
e
5 µm
0 10 20 30
Sec
C
GFP-Myosin
5 µm
D
70%
60%
50%
40%
30%
20%
10%
0%
-10%
-20%
-30%
equator
outside equator

transient increases (Figure 3.4A, and Supplemental Video 3.2). No such domains were observed with cells expressing GFP-actin or GFP alone. To visualize more directly myosin intensity dynamics and to normalize against the local concentration, TDM was applied, which calculates the rate of temporal differential, $(I_{t+\Delta t} - I_t)/(I_{t+\Delta t} + I_t)/\Delta t/2$, with pairs of images I_t, $I_{t+\Delta t}$ separated temporally by Δt. This quantity approximates the rate of percentage change in intensity. The resulting images were rendered in color, with bright orange marking regions of strong proportional increases in intensity and bright blue marking regions of strong decrease (N = 31; Figure 3.4A, and Supplemental Video 3.2). TDM revealed strong assembly domains of myosin up to 10 μm in diameter throughout the cortex. These domains lasted typically 15-20 seconds, during which some of them traveled across the cortex (Figure 3.4A). These observations indicate that myosin assembly was not confined to the equatorial region (Lucero *et al.*, 2006), although the equatorial region may have a higher net assembly activity than elsewhere.

TDM also revealed suppression of disassembly/dissociation activities along the equator. While a strong phase of assembly outside the equator was typically followed by an equally strong phase of disassembly, assembly along the equator was followed by a neutral phase (Figure 3.4B, and Supplemental Video 3.2), when the intensity remained steady or increased slowly. Therefore, a net increase in equatorial myosin may be achieved through a rectifier-like effect, by allowing assembly or association on the entire cortex while suppressing disassembly or dissociation along the equator (Figure 3.4B). The regulation of myosin disassembly or dissociation may thus play a crucial role in equatorial recruitment.

Figure 3.4 Random domains of myosin assembly/association and inhibition of myosin disassembly/dissociation along the equatorial cortex. TDM reveals highly dynamic domains of myosin assembly/association and disassembly/dissociation throughout the cortex during early cytokinesis (A). Regions of assembly/association are shown in orange and regions of disassembly/dissociation shown in blue. During the assembly of the equatorial band, disassembly is suppressed along the equator (B), such that strong increases in intensity along the equator are followed by weak increases or steady intensities (A, arrows, and B), whereas strong increases outside the equator are followed by strong decreases (A, arrowheads, and C). Yellow boxes (A) indicate the regions plotted (green curves in B, C). Green, red, blue curves represent the rate of intensity change and the average intensity in equatorial or polar regions of 20x20 pixels in three individual cells (B, C). The average intensity at t=0 is set as 100 arbitrary units. Supplemental Videos 3.2 shows the corresponding movie.

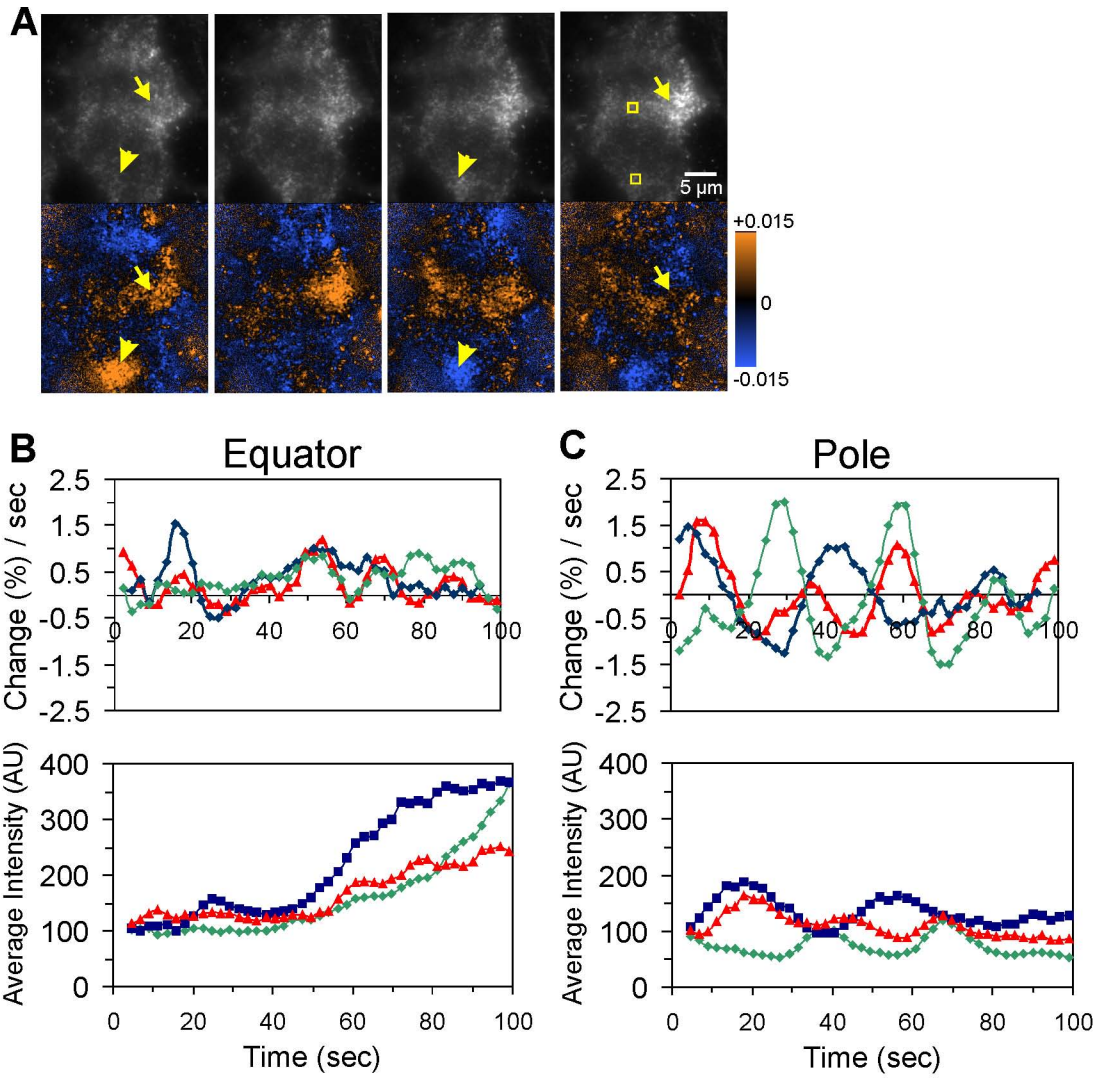
A
5 µm
+0.015
0
-0.015
B
Equator
C
Pole
Change (%) / sec
Average Intensity (AU)
Time (sec)
2.5
1.5
0.5
-0.5
-1.5
-2.5
400
300
200
100
0
0
20
40
60
80
100

Cortical myosin is affected in different ways by small GTPase Rho, Rho kinase, myosin light chain kinase, and its own ATPase activities during cytokinesis

Cortical dynamics of myosin is likely affected by its ATPase and self-assembly activities, which are in turn regulated by rMLC by a number of kinases including MLCK and ROCK (Bresnick, 1999; Poperechnaya *et al.*, 2000; Fukata *et al.*, 2001; Chew *et al.*, 2002; Matsumura, 2005). Y-27632, an inhibitor of ROCK, delayed cytokinesis as reported previously (Kosako *et al.*, 2000). The formation of equatorial myosin band appeared uninhibited (Figure 3.5A). However, time-lapse movies and kymographs indicated that equatorial myosin dots were surprisingly stable in Y-27532 treated cells (Figure 3.5A). Myosin dots outside the equator became sparse and highly transient compare to those in control cells shown in Figure 3.3, suggesting that they failed to associate stably with the cortex (Figure 3.5A; Supplemental Video 3.3). In addition, TDM analysis showed a strong inhibition of dynamic myosin domains throughout the cortex (Figure 3.5D). Injection of C3 transferase (a Rho inhibitor), unlike Y-27632 treatment, caused complete inhibition of the recruitment of myosin dots along the equator (Figure 3.5C, Figure 3.6; (O'Connell *et al.*, 1999; Kamijo *et al.*, 2006), suggesting that ROCK is not the only effector of Rho that regulates equatorial myosin recruitment. ML-7, an inhibitor of MLCK, caused a delay in cytokinesis without an apparent effect on cortical myosin dots along or outside the equator (Supplemental Video 3.4).

Since C3 and Y-27632 presumably inhibit myosin ATPase by inhibiting rMLC phosphorylation, their effects were compared with the effect of (-)-blebbistatin, a potent myosin ATPase inhibitor. Blebbistatin caused an increase in the intensity of myosin dots throughout the cortex (Figure 3.5B, Supplemental Video 3.5), by 97% along the equator

Figure 3.5 Different effects of inhibitors of ROCK, Rho, and myosin ATPase on cortical myosin dynamics during cytokinesis. Myosin localization along the equator appears uninhibited in a cell treated with Y-27632, a ROCK inhibitor (A, left panel, arrows indicate equator). Kymograph analysis indicates that myosin dots in the equatorial region become surprisingly stable (A, kymograph 1, right upper panel), while dots away from the equator become weak and highly unstable (A, kymograph 2, right bottom panel) compared with those in similar regions of control cells (Figure 3.3B, b and e). Supplemental Video 3.3 shows the corresponding movie. Injection of C3 transferase, a Rho GTPase inhibitor, in contrast, causes a strong inhibition of myosin localization along the equator (C, arrows indicate equator). (-)-Blebbistatin, a myosin ATPase inhibitor, increases cortical myosin intensity both inside and outside the equatorial region (B, arrows indicate equator). Supplemental Video 3.4 shows the corresponding movie. TDM analysis shows the strong inhibition of intensity fluctuations by Y-27632 (D), in contrast to the waves seen in control cells (Figure 3.4B and C).

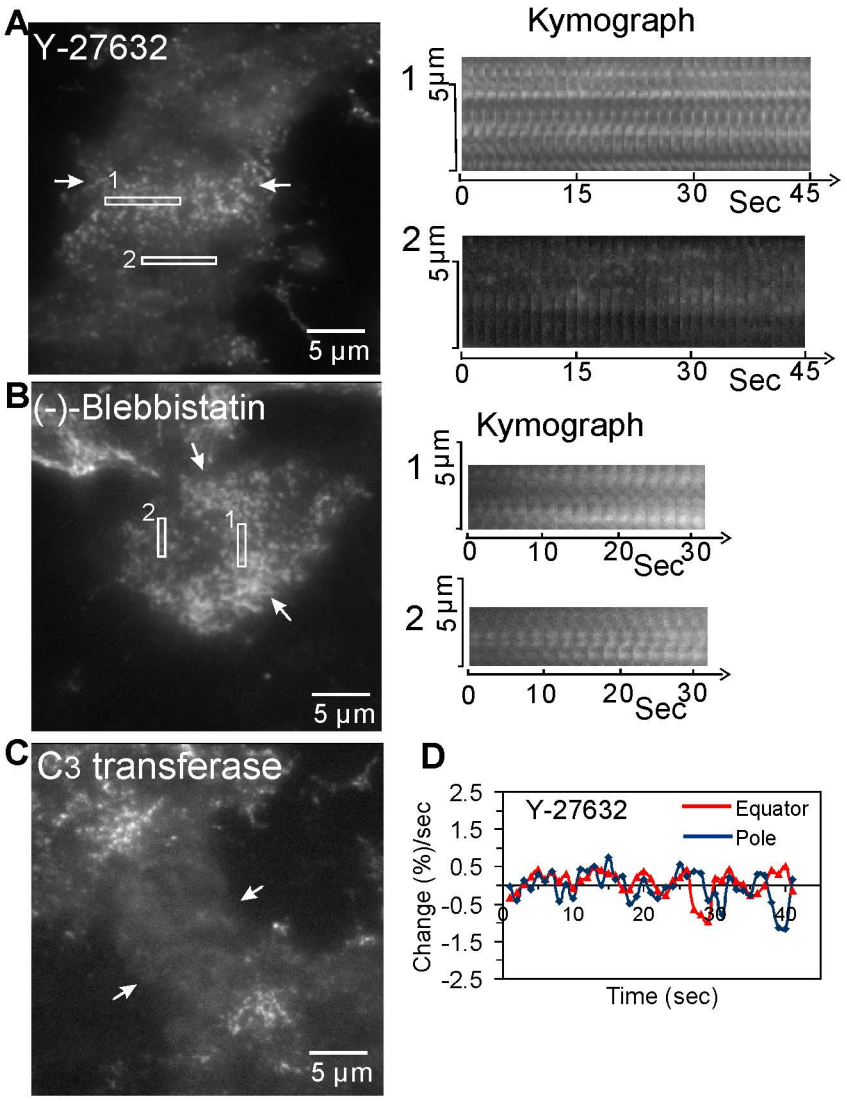
A
Y-27632
1
2
5 µm
Kymograph
1
5µm
0
15
30
Sec
45
2
5µm
0
15
30
Sec
45
B
(-)-Blebbistatin
2
1
5 µm
Kymograph
1
5µm
0
10
20
Sec
30
2
5µm
0
10
20
Sec
30
C
C3 transferase
5 µm
D
Y-27632
Equator
Pole
Change (%)/sec
2.5
1.5
0.5
-0.5
-1.5
-2.5
0
10
20
30
40
Time (sec)

Figure 3.6 TIRF-M time-lapse sequence of GFP-myosin in NRK cell injected with C3, a Rho inhibitor. The cell shows strong inhibition of myosin localization along the equator (arrows indicate the equator).

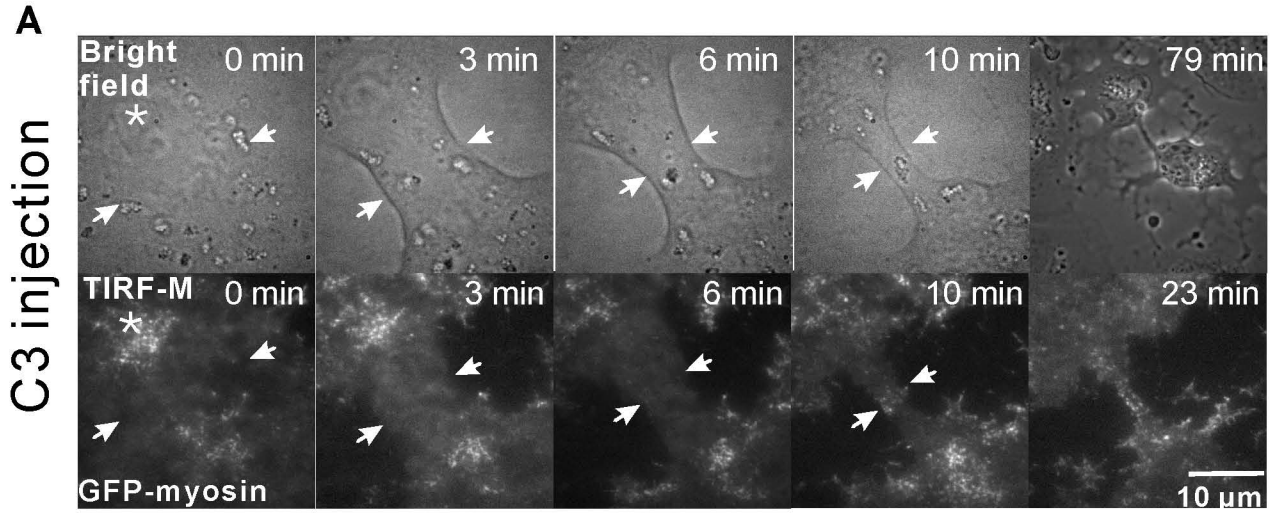
A
C3 injection
Bright field
0 min
3 min
6 min
10 min
79 min
TIRF-M
0 min
3 min
6 min
10 min
23 min
GFP-myosin
10 µm

Figure 3.7 Recruitment of myosin to the equator in cells treated with latrunculin B. TIRF-M of GFP-myosin shows the recruitment to the equatorial cortex despite the inhibition of cytokinesis and disassembly of actin filaments (A; asterisk and boxed region indicate the equator in a tri-polar cell). However, the myosin band begins to widen at about 10 min after anaphase onset, and eventually disperses at about 25 min after anaphase onset, indicating that F-actin may be involved maintaining myosin organization in the furrow. Time is indicated as minutes:seconds from anaphase onset. Kymograph analysis shows that myosin dots persist for minutes (B, arrows indicate equator, white rectangular box indicates the region analyzed). Supplemental Video 3.6 shows the corresponding movie.

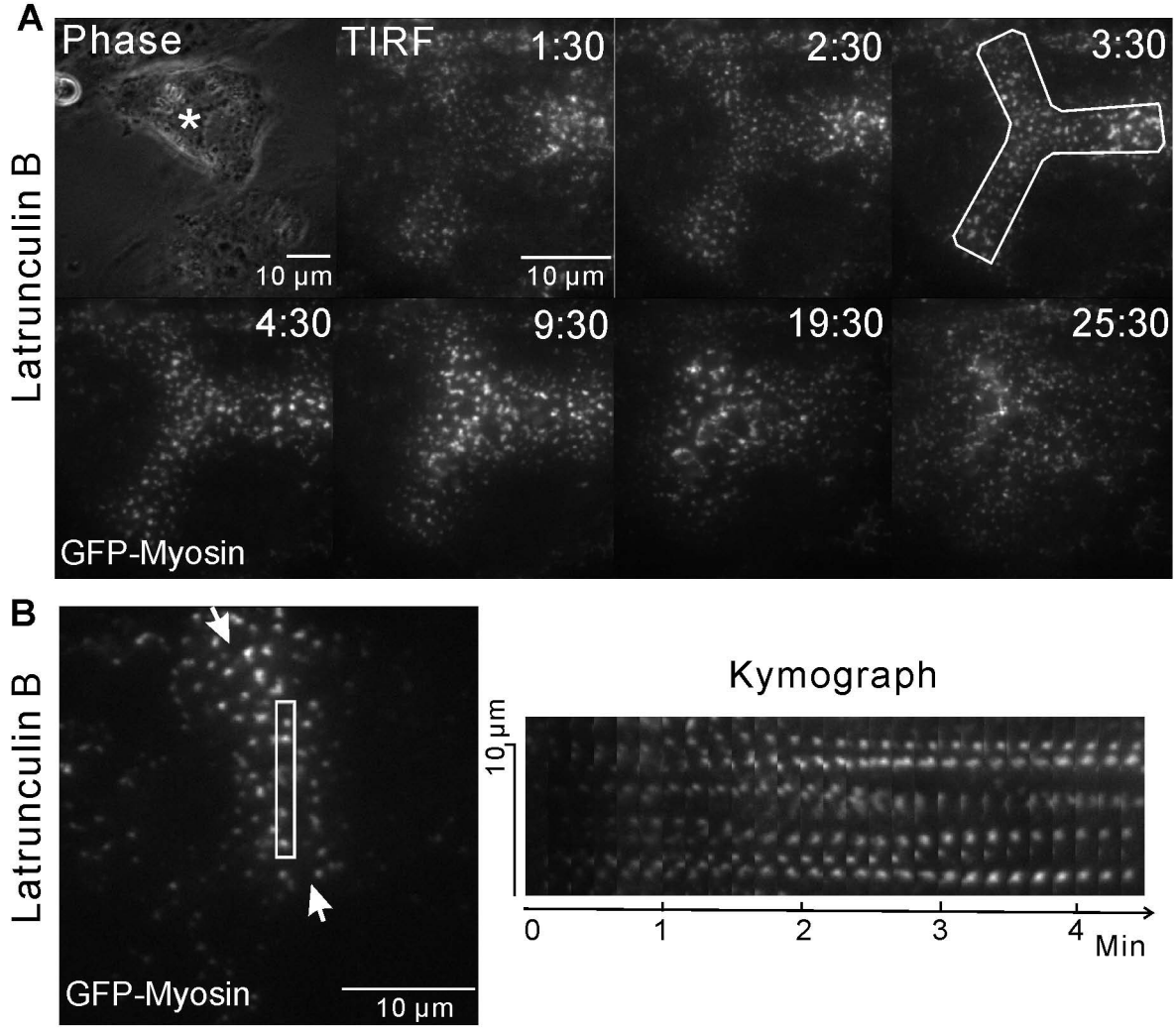
A
Latrunculin B
Phase
TIRF
1:30
2:30
3:30
4:30
9:30
19:30
25:30
10 µm
10 µm
GFP-Myosin
B
Latrunculin B
GFP-Myosin
10 µm
Kymograph
10 µm
0
1
2
3
4
Min

and 71% outside the equator during a 30 second period in early cytokinesis. The different effects between (-)-blebbistatin and Rho/ROCK inhibitors suggest that myosin ATPase activity and rMLC phosphorylation play distinct roles in cortical myosin recruitment. Also relevant was the previous demonstration that equatorial myosin recruitment took place in yeast, *Drosophila* and HeLa cells treated with latrunculin B (Wu *et al.*, 2003; Dean *et al.*, 2005; Kamijo *et al.*, 2006), which induces depolymerization of actin filaments and thereby inhibits the actomyosin ATPase. This was also the case for NRK cells (Figure 3.7, and Supplemental Video 3.6). However, the equatorial myosin band gradually widened over about 20 minutes after anaphase onset, suggesting that acto-myosin interactions play a role in restricting the equatorial myosin localization (Figure 3.7).

Recruitment of equatorial actin involves a combination of myosin motor-dependent fluxes and de novo assembly

The delay of equatorial actin recruitment relative to that of myosin suggested that actin and myosin may follow different pathways (Figure 3.2B). To observe directly the equatorial recruitment of actin, I collected time-lapse movies of dividing cells expressing GFP-actin or mCherry-actin. In contrast to myosin, actin filaments showed a striking flux toward the equator during cytokinesis (observed in 20 cells; Figure 3.8A and B, Supplemental Videos 3.7 and 3.8), at an estimated average speed of 2.1±0.6 μm/min based on the slopes of kymographs (Figure 3.9B). The flux was unlikely to reflect the movement of the entire cortical actin structure, since some actin structures moved to the equator while others remained stationary (Figure 3.8B). In addition, small actin

structures were observed to dissociate from large patches and move into the furrow, suggesting that actin disassembly or severing, rather than a global collapse of the cortical network, may be involved in the generation of the flux (Supplemental Video 3.7). Moreover, STICS analysis indicated heterogeneous speeds and movement patterns, and juxtaposition of directional and random movements (Figure 3.8C), further arguing against global movement of a crosslinked cortex.

The long-range, directed movement of actin filaments implied the involvement of motor-dependent forces. To determine if myosin motor activities were responsible for the actin flux, I investigated the effect of (-)-blebbistatin. The treatment with (-)-blebbistatin immediately inhibited the actin flux, while (+)-blebbistatin (an inactive form of blebbistatin as negative control) had no effect (Figure 3.9A; Supplemental Video 3.9). The slopes in the kymographs indicate an average flux speed of 2.1 μm/min in control cells, and close to zero in (-)-blebbistatin treated cells (Figure 3.9B), suggesting that myosin motor activities were critical for the actin flux. However, equatorial concentration of actin filaments took place despite the inhibition of actin flux (Supplemental Video 3.9 and 3.10). TDM further confirmed the persistence of actin assembly activities along the equator in the presence of (-)-blebbistatin (Figure 3.10). Therefore both filament flux and de novo assembly were involved in actin recruitment along the equator.

Figure 3.8 Striking actin flux toward the equator during early cytokinesis. Cells expressing GFP-actin or mCherry-actin show striking actin flux toward the equator during early cytokinesis (A, Supplemental Videos 3.7 and 3.8). White rectangular boxes indicate the regions analyzed in kymographs and arrows indicate the equator (A). Kymograph analysis (B) and STICS analysis (C) show some actin structures on the cortex move toward equator (B, panel 1 and 3), while others do not move (B, panel 2). Thus the flux does not represent global cortical movement. The scale bar also represents a speed of 0.22 μm/sec in STICS (C)

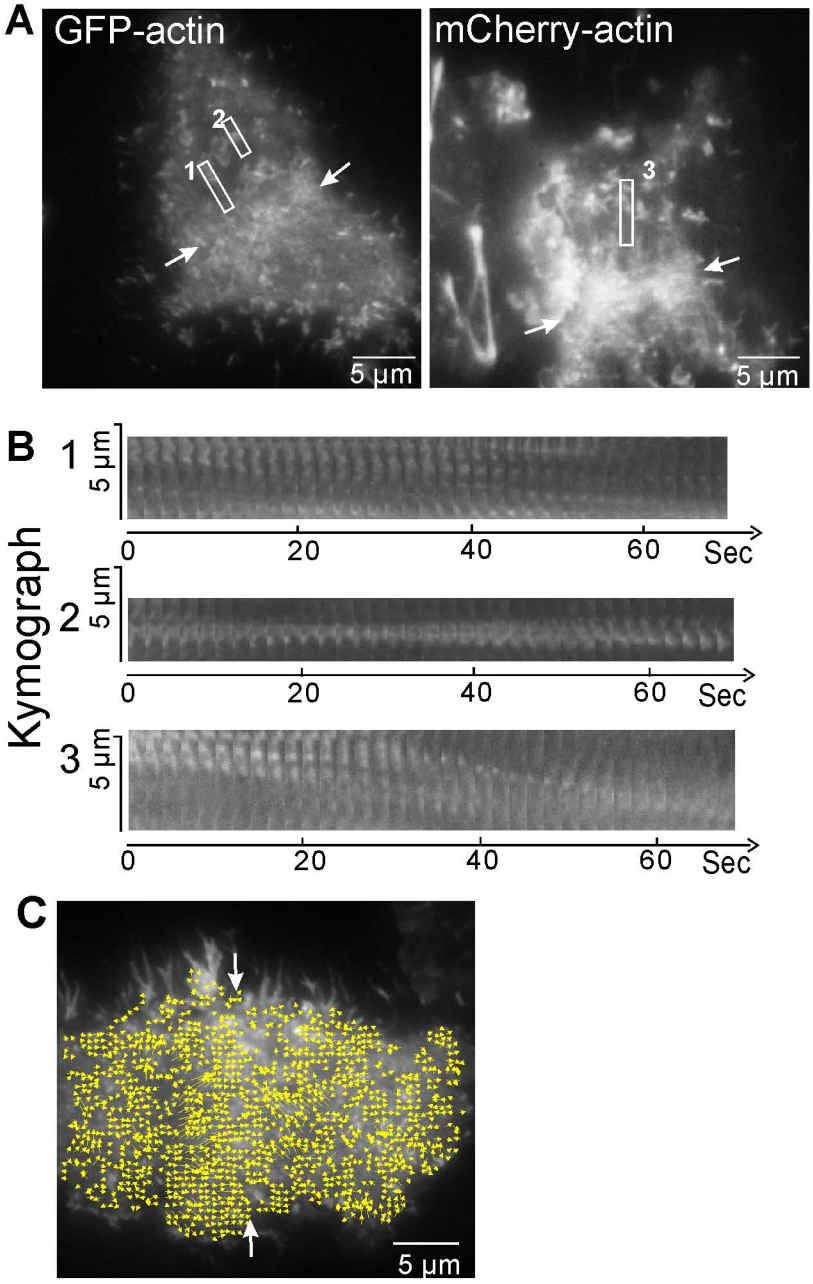
A
GFP-actin
mCherry-actin
1
2
3
5 μm
5 μm
B
Kymograph
1
2
3
5 μm
0
20
40
60
Sec
C
5 μm

Figure 3.9 Requirement of myosin motor activity for the actin flux. Treatment with active (-)-blebbistatin abolishes actin flux (A, bottom panel), while treatment with the inactive isomer (+)-blebbistatin has no effect (A, upper panel), as suggested by both STICS (A, left panels) and kymographs (A, right panels). White rectangular boxes indicate the regions analyzed by kymographs and arrows indicate the equator (A, middle panel, and Supplemental Video 3.9). The slopes in the kymographs indicate an average flux speed of 2.1 μm/min in control cells, and close to zero in (-)-blebbistatin treated cells (B; n=19 for the control and n=8 for blebbistatin; error bars indicate the standard deviation).

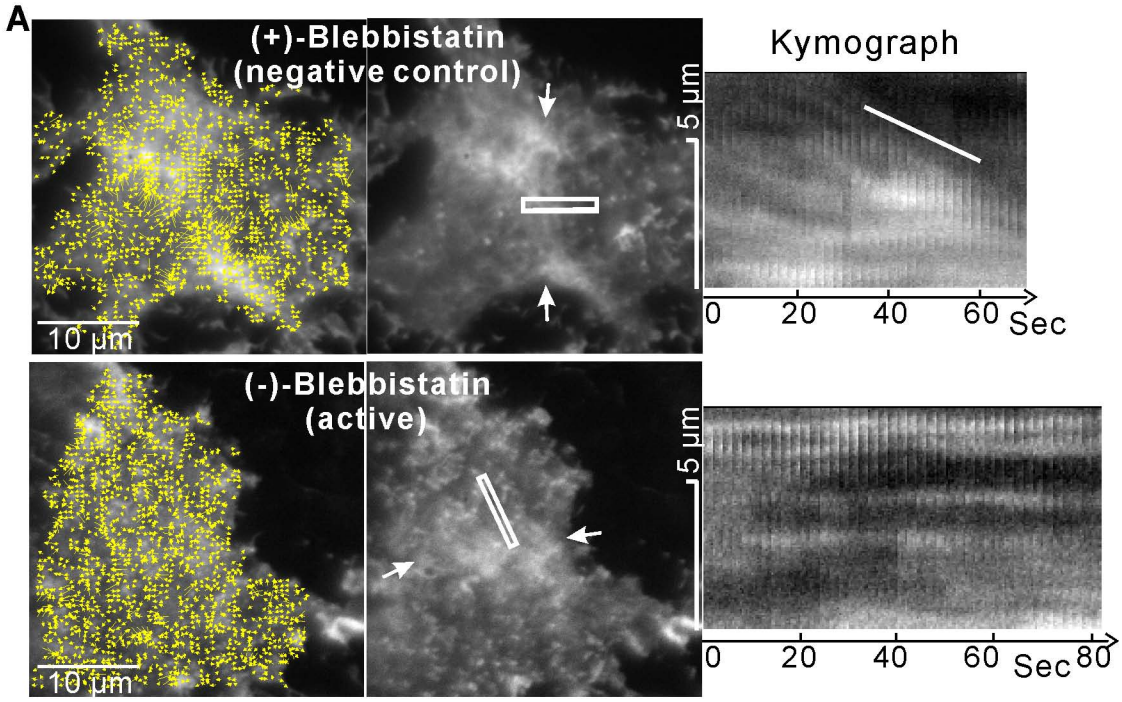
A
(+)-Blebbistatin
(negative control)
10 μm
Kymograph
5 μm
0
20
40
60
Sec
(-)-Blebbistatin
(active)
10 μm
5 μm
0
20
40
60
Sec
80

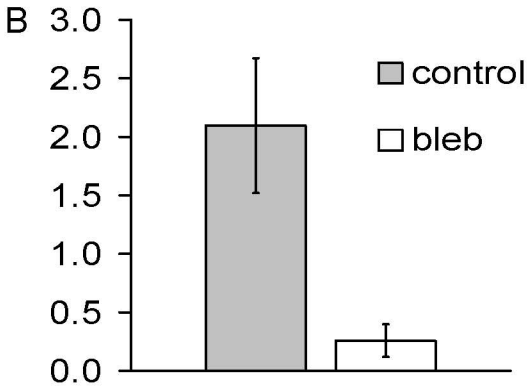
B
3.0
2.5
2.0
1.5
1.0
0.5
0.0
control
bleb

Figure 3.10 Involvement of both myosin motor-dependent fluxes and de novo assembly in the recruitment of equatorial actin. TDM of cell treated with active (-)-blebbistatin shows inhibition of actin flux and cytokinesis, while the equatorial region shows net assembly (A, arrows indicate equator). Plots of percentage intensity change per second (B, left panel) or average intensity in regions of 20x20 pixels (B, right panel) show a broad peak of assembly activities along the equator during early cytokinesis (B, red curve), while the polar region shows fluctuating values around the baseline (B, blue curve). The regions plotted are indicated by yellow boxes in the corresponding TIRF-M image (A, right panel). The average intensity at t=0 is set as 100 arbitrary units. Supplemental Video 3.10 shows the corresponding movie.

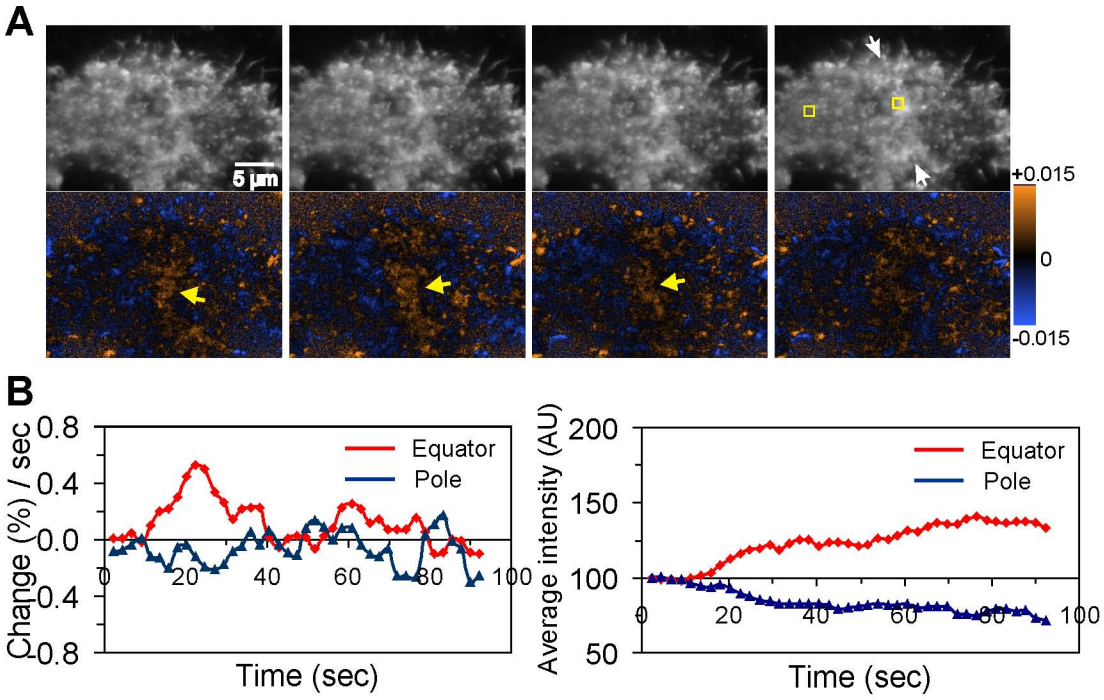
A
5 µm
+0.015
0
-0.015
B
Change (%) / sec
0.8
0.4
0.0
-0.4
-0.8
0
20
40
60
80
100
Time (sec)
Equator
Pole
Average intensity (AU)
200
150
100
50
0
20
40
60
80
100
Time (sec)
Equator
Pole

Discussion

Equatorial concentration of actin and myosin represents a common feature of cytokinesis seen from yeast to mammalian cells. Despite the variability in the extent of concentration, likely due to the feedback from cortical resistance to ingression and the balance between assembly and disassembly activities (Fishkind and Wang, 1995), it is generally believed that the recruitment process holds an important key to the understanding of the mechanism of cytokinesis. For example, the polar relaxation hypothesis predicts that the entire cortical structures should move toward the equator, due to the weak forces in the polar region relative to the strong contractions along the equator (White and Borisy, 1983). In contrast, some versions of the equatorial contraction mechanism emphasize a de novo mechanism for equatorial structural assembly (Wu *et al.*, 2006), while other versions incorporate cortical flow as part of an assembly process (He and Dembo, 1997). However, due to the lack of high-resolution images depicting the recruitment process in mammalian cells, there has been no definitive evidence for these proposed mechanisms. The clarity of images provided by TIRF-M has allowed me to determine unambiguously the behavior of cortical actin and myosin during early cytokinesis.

Equatorial recruitment of myosin in early cytokinesis does not involve cortical flow

While dot-like structures of cortical myosin have been observed during cytokinesis in fixed samples by confocal microscope (Maupin *et al.*, 1994), little is known about how they become concentrated along the equator. The present results, showing no detectable, long-range flow of myosin dots toward the equator, argued against the cortical flow

hypothesis for myosin recruitment and supported either the assembly of myosin minifilaments from cytoplasmic subunits or recruitment of preassembled minifilaments. Although the polar cortex showed a net loss of myosin dots, myosin appeared to be released into cytoplasm first and recruited to the equator. This shift in the balance of myosin cortical association may involve differential interactions of polar and equatorial cortices with astral microtubules (Werner *et al.*, 2007).

My results appear to contradict previously reported fluxes of myosin in mammalian cells (DeBiasio *et al.*, 1996), and in *Dictyostelium* (Yumura, 2001). However, the present observations were focused on early assembly events of equatorial cortex. During the subsequent phase of active ingression, I did observe some limited movements of myosin dots on the equatorial cortex and in the immediately adjacent region, which likely reflect contractile activities and may explain previous observations of myosin movements (DeBiasio *et al.*, 1996). In addition, different organisms may adopt different mechanisms of myosin recruitment, as suggested by the multiple mechanisms of cytokinesis in motile *Dictyostelium* cells (Uyeda *et al.*, 2004).

Equatorial recruitment of actin involves a combination of cortical flow and de novo assembly

In contrast to myosin, cortical actin showed a striking flux toward the equator, consistent with previous observations at a limited resolution using conventional optics and microinjected fluorescent phalloidin (Cao and Wang, 1990b). In addition, the flux took place in discrete domains flanking the equator, and at least part of the moving structures appeared to be generated by severing and/or disassembling existing actin

structures, suggesting that the flux was an active, selective process rather than global cortex movement as a result of force balance.

Treatment of blebbistatin abolished the actin flux and inhibited actin turnover, but did not inhibit actin concentration in the equator (Guha *et al.*, 2005; Murthy and Wadsworth, 2005), suggesting that the flux was driven by myosin motor activities and that there were additional, flux-independent mechanisms, likely de novo assembly as suggested in other systems (Noguchi and Mabuchi, 2001; Pelham and Chang, 2002; Severson *et al.*, 2002; Wu *et al.*, 2006). Myosin may be involved in both processes, by providing forces for the flux and by facilitating the turnover of actin cortex to generate the sources of flux. Since blebbistatin also completely inhibited furrow ingression, it is possible that cytokinesis requires not only an equatorial acto-myosin band but also actin flux and/or turnover. In addition, although the major events of cytokinesis take place along the equator, the complex picture presented by TIRF-M suggested that the process may involve the entire cortex.

Equatorial myosin recruitment involves the regulation of both assembly and disassembly processes

Dynamic cytoskeletal structures are maintained by a balance between assembly and disassembly activities. Previous immunostaining studies have shown a concentration of mono- and di-phosphorylated rMLC along the equator, which is known to activate the myosin ATPase and promote the assembly of filamentous myosin structures (Matsumura *et al.*, 1998; Matsumura *et al.*, 2001). These observations were often interpreted as suggesting an increase in the rate of myosin assembly or cortical association along the

equator. However, equatorial rMLC phosphorylation, and myosin structures, may be stimulated equally effectively by decreasing the rate of disassembly or dissociation from the equatorial cortex, as was suggested by the requirement of regulated myosin phosphatase activities in cytokinesis (Matsumura, 2005).

Time-lapse TIRF-M and TDM revealed surprisingly active domains of cortical myosin assembly/association throughout the cell cortex immediately after anaphase onset. These domains were not detected in previous studies, because without TIRF-M, their contrast against the strong cytoplasmic signals was likely to be very low. In addition, the transient, random nature of these domains likely made them very difficult to notice in fixed cells. The global presence of these assembly domains suggested that assembly signals for myosin were not confined to the equatorial region (Lucero *et al.*, 2006).

Previous studies showed that the primary function of ROCK during cytokines is to elevate the phosphorylation of rMLC (Dean and Spudich, 2006). The strong inhibition of dynamic domains of cortical myosin assembly by Y-27632, as shown in the present study, suggested that ROCK and ROCK-mediated phosphorylation of rMLC were involved in the recruitment of myosin throughout the cortex. However, the presence of equatorial myosin band despite the inhibition of ROCK suggested a second, ROCK-independent pathway that directly recruited myosin to the equatorial cortex. .

TDM analysis further revealed local inhibition of myosin disassembly/dissociation along the equator, which likely contributed to the build up of myosin concentration. Unexpectedly, the stability of equatorial myosin in the presence of Y-27632 suggested that the stabilization involved a mechanism independent of ROCK-induced direct rMLC phosphorylation or inhibition of myosin phosphatase (Fukata *et al.*, 2001), while the

turnover was dependent on ROCK. Furthermore, actin filaments may play a role in the stability of myosin, as suggested by the gradual expansion of the equatorial myosin band in latrunculin treated cells. Other molecules such as anillin have also been implicated in the recruitment of myosin, possibly by stabilizing myosin association along the equator (Straight *et al.*, 2005).

The effects of blebbistatin on cortical myosin distribution and dynamics were strikingly different from those of Y-27632 or C3. Inhibition of myosin ATPase activity by blebbistatin appeared to inhibit cortical myosin disassembly/dissociation without affecting cortical myosin assembly/association, indicating that the ATPase activity is not required for its cortical association but may be required for its turnover. In contrast, C3 caused strong inhibition of equatorial myosin recruitment, suggesting that the primary effect of Rho on myosin was not the regulation of ATPase activities, but possibly its self assembly, disassembly, and/or cortical association.

In conclusion, many previous models of cortical ingression involved global, coupled movements of actin and myosin filaments into the equatorial region. The present study showed that, while a prominent myosin-dependent actin flux did occur during the cytokinesis of NRK cells, the movement was by no means global and no such movement was detectable for myosin. In addition, the formation of the equatorial actin band involved a second, myosin-independent, de novo assembly process. These results support an active mechanism that promotes structural organization at the equator, rather than a passive mechanism as a consequence of differential cortical contractile activities. Moreover, the discovery of dynamic domains of myosin assembly throughout the cortex,

combined with a localized suppression of myosin disassembly/dissociation along the equator, suggests that the spatial and temporal control of cytokinesis may involve the regulation of both assembly and disassembly activities.

Supplemental Materials

Supplemental Video 3.1. TIRF-M of an NRK cell expressing GFP-nonmuscle myosin IIA heavy chain during the assembly of equatorial cortex. No directed flow of cortical myosin is detectable. Enlarged view of the equatorial region is shown to the right.

Supplemental Video 3.2. TIRF-M and the corresponding TDM of GFP-myosin in an NRK cell during the assembly of the equatorial cortex. Dynamic domains of myosin assembly/association appear throughout the cortex. Some assembly domains appear to travel across the cell cortex. The total duration of recording is 87 seconds.

Supplemental Video 3.3. Recruitment of GFP-myosin to the equator in cell treated with Y-27632. TIRF-M shows that myosin in the equatorial region is very stably associated with cortex, in contrast to dots outside the equator. The total duration of recording is 66 seconds.

Supplemental Video 3.4. Equatorial recruitment of GFP-myosin in a cell treated with ML-7. Cytokinesis is delayed. The total duration of recording is 3.75 minutes.

Supplemental Video 3.5. Equatorial recruitment of GFP-myosin in a cell treated with (-)-blebbistatin. Cortical myosin intensity shows steady increase both in and outside the equatorial region, while cytokinesis is inhibited. The total duration of recording is 34 seconds.

Supplemental Video 3.6. Equatorial recruitment of GFP-myosin in a cell treated with latrunculin B, despite the inhibition of furrow ingression. Equatorial myosin dots appear to scatter over a wide region than in control cells. The total duration of recording is 4.5 minutes.

Supplemental Video 3.7. TIRF-M of an NRK cell expressing GFP-actin during the assembly of equatorial cortex, showing dramatic fluxes of actin filaments toward the equator.

Supplemental Video 3.8. TIRF-M of an NRK cell expressing mCherry-actin during the assembly of equatorial cortex, showing dramatic fluxes of actin filaments toward the equator, as well as active ruffles of a neighboring cell. The total duration of recording is 70 seconds.

Supplemental Video 3.9. TIRF-M of NRK cells expressing mCherry-actin treated with (+)-blebbistatin (negative control, left) or (-)-blebbistatin (myosin ATPase inhibitor, right). (+)-blebbistatin has no effect on actin flux, while (-)-blebbistatin abolishes actin flux. Despite the inhibition of flux, equatorial actin concentration remains unaffected.

Supplemental Video 3.10. TIRF-M and the corresponding TDM of mCherry-actin in an NRK cell treated with (-)-blebbistatin. Equatorial band appears despite the inhibition of actin flux. Bands of de novo assembly activities are visible in the TDM image along the

equator during the first half of the recording. The total duration of recording is 75 seconds.

Chapter IV - Post-mitotic Spreading: Role of Retraction Fibers

Abstract

Mitotic rounding and post-mitotic spreading are important events in animal cell mitosis. It has been noticed that mitotic cells leave retraction fibers on the substrate during rounding, however, little is known about the function of these fibers. In this study, I have focused on the role of retraction fibers in post-mitotic spreading. I found that retraction fibers transform directly into filopodia during post-mitotic spreading. Cells with retraction fibers showed increased speed in post-mitotic spreading compared to cells without retraction fibers. In addition, micromanipulation studies show retraction fibers may guide the direction of post-mitotic spreading. I further demonstrated that focal adhesion proteins are present at the tips of retraction fibers, where they may provide nucleation sites for focal adhesion assembly to help rapid restoration of substrate adhesions. These findings may suggest a general mechanism of adherent cells to facilitate post-mitotic spreading and to quickly reoccupy their previous territory after mitosis.

Introduction

Many adhesive cells form focal adhesions on substrates during interphase (Abercrombie and Dunn, 1975). These adhesions help cells to anchor on the substrate and maintain a spread morphology. During cell migration, focal adhesions form exclusively or predominantly in protrusive regions (Sheetz *et al.*, 1999). Some of them mature and persist during migration, showing little mobility relative to the substrate. When finally falling behind the tail region, persisting focal adhesions may become connected with the cell body with a fine thread of cytoplasm referred to retraction fibers. Some focal adhesions disassemble eventually, allowing the absorption of the retraction fiber into the cell body, while others become detached from the cell body as adhesive fragments on the substrate. This phenomenon has been observed with various cell types, such as fibroblasts, macrophages, and keratinocytes (Chen, 1981; Kirfel *et al.*, 2003; Wolf *et al.*, 2003).

These tiny retraction fibers are not readily detectable under phase contrast microscopy, but may be highlighted using approaches such as interference reflection microscopy (IRM), atomic force microscopy (AFM), or electron microscopy (EM) (Zimmermann *et al.*, 1999; Richter *et al.*, 2000; Kirfel *et al.*, 2003). However, while these approaches have allowed discovery of retraction structures in more cell types, very little is known about their physiological functions. It is generally speculated that retraction fibers are involved mainly in the maintenance of pre-existing substrate adhesions rather than the formation of new adhesion sites.

Equally interesting, retraction fibers are found during mitosis, when cells undergo drastic changes in cytoskeletal structures including the disassembly of stress fibers and focal adhesions, detachment of cells from the substrate, and cell rounding (Yamaguchi *et*

al., 1997; Yamakita *et al.*, 1999). Under favorable optical conditions, retraction fibers may be observed surrounding mitotic cells similar to those in the tail region of migrating interphase cells (Harris, 1973). After mitosis, adherent cells undergo rapid respreading, re-establishing their substrate adhesions and restoring the spread interphase morphology. These observations, however, have attracted little attention and shed little light on the function of mitotic retraction fibers. In this study, I have probed the functional role of retraction fibers in post-mitotic spreading and demonstrated that they guide and facilitate post-mitotic spreading. Cell with retraction fibers showed increased speed in post-mitotic spreading toward regions occupied by retraction fibers compared to those without retraction fibers. In addition, traction fibers appeared to function as nucleation sites that mediated direct reformation of focal adhesions. These findings may suggest a mechanism that facilitates rapid restoration of interphase morphology and reoccupation of previous cell territory after mitosis exit.

Materials and Methods

Cell Culture and Transfection

A subclone of Normal Rat Kidney epithelial cells (NRK-52E; American Type Culture Collection, Rockville, MD) was grown on glass coverslips in Kaighan's modified F12 medium (Sigma, St. Louis, MO) supplemented with 10% fetal calf serum (JRH Biosciences, Kansas City, MO), 1 mM L-glutamine, 50 µg/mL streptomycin and 50 U/mL penicillin (Gibco, Carlsbad, CA). Cells were maintained at 37^{o}C in a humidified atmosphere containing 5% CO_2. Transient transfection of NRK epithelial cells was performed by nucleofection using the Amaxa nucleofector and kit R (Amaxa, Gaithersburg, MD), following manufacturer's protocol. After transfection, cells were plated on glass coverslips and cultured overnight before imaging. Red fluorescent protein (RFP)-zyxin was constructed by recloning the enhanced green fluorescent protein (EGFP) construct (provided by Dr.Wehland J, Germany) into the pDsRed1-N1vector (Clontech, Palo Alto, CA).

Micromanipulation and data analysis

The micromanipulation study was conducted using glass capillary tubing that was pulled into needles with a vertical micropipette puller (David Kopf Instruments, Tujunga, CA). The tip of the needle was then melted and shaped with a microforge (Narishige, East Meadow, NY). A micromanipulator (Leitz, Wetzlar, Germany) was used to control the needle to gently remove neighboring cells from a mitotic cell without affecting the mitotic cell. Time lapse images were recorded during post-mitotic spreading. To analyze the data, a straight line was drawn along the long axis of the mitotic cell imparting the

cell into two equal halves, with retraction fibers on one side of the line and no retraction fibers on the other side. The spread area on both sides of the line was then measured 5 minutes after post-mitotic spreading starts, and the ratio of the spread area was calculated. The spreading rate was calculated by dividing the spread area with spreading time. To study post-mitotic spreading without retraction fibers, mitotic cells were shaken off and replated on coverslips coated with fibronectin (100ug/ml) that allows most cells attach the substrate within 10 minutes.

Immunofluorescence

Cells were fixed in 4% paraformaldehyde in cytoskeletal buffer for 10 minutes before staining. Samples were blocked with 1% bovine serum albumin/PBS for 15 min at room temperature, then incubated for 45 minutes at 37^{o}C with 1:100 dilution of primary antibodies against paxillin (Santa Cruz Biotechnology, Santa Cruz, CA) or vinculin (clone VIN11-5; Sigma-Aldrich).

Microscopy and Data Collection

Phase contrast images were collected with either a Zeiss Axiovert-10 or Axiovert-200M inverted microscope (Thornwood, NY), equipped with a 40x, N.A. 0.65 or a 100x, N.A. 1.30 phase contrast Plan-Neofluar objective lens. Interference reflection microscopy (IRM) was performed by placing a half-reflecting mirror in the epi-illumination path and closing down the epi-illumination aperture diaphragm, using a Zeiss Axiovert-200M microscope equipped with a 100× N.A. 1.30 NeoFluar phase contrast objective lens. Fluorescence images were collected with a cooled CCD camera

(Model NTE/CCD-512-EBFT, Princeton Instrument, Trenton, NJ, or Model DV-887-DCS-BV, Andor Technology, Belfast, UK) and subtracted with a dark count image. Except for linear adjustments across the entire image to optimize the display, the images were unaltered. Data acquisition and analyses were performed with ImageJ (NIH).

Results and Discussion

NRK cells leave retraction fibers on the substrate during mitotic rounding

Normal rat kidney (NRK) epithelial cells cultured on glass coverslips showed numerous retraction fibers during early stages of mitotic rounding (Figure 4.1A a-c). These fibers became difficult to detect with phase contrast optics during metaphase, appearing predominantly as little phase-dense dots (Figure 4.1A d) that spanned the original area before cell rounding. Under IRM, they appeared as fine fibers surrounding some cells emanating from the cell body and forming a branched network (Figure 4.1B b and d), suggesting that these fibers were in close contact with the substrate. Similar retraction fibers were also observed in cells cultured on coverslips coated with fibronectin or type I collagen (not shown).

Filopodia emerges along retraction fibers during post-mitotic spreading

By recording time-lapse images of cells undergoing post-mitotic spreading, I found that spreading involved rapid expansion and extension of the cytoplasm toward the tips of retraction fibers, showing filopodia-like structures along retraction fibers during the transient state (Figure 4.2A, Supplemental video 4.1).

Retraction fibers were unlikely to be essential for cell spreading, as indicated by the ability of trypsin-detached cells to respread without retraction fibers. However, respreading of trypsinized cells is substantially slower, taking typically hours to reach a steady state (unpublished observations, (Bereiter-Hahn *et al.*, 1990)), while post-mitotic spreading may be complete in less than 20 minutes, suggesting that retraction fibers may play a role in facilitating post-mitotic spreading. Measurements of the rate of post-

Figure 4.1 NRK cells leave retraction fibers on the substrate during mitotic rounding. Time lapse sequence using phase contrast optics shows how a mitotic cell leaves retraction fibers on the substrate upon rounding (A). Except for the tips, some fibers become difficult to detect and appear to be severed from the cell body during metaphase. The fibers in two different cells are more readily detectable with interference reflection optics (B, right panel), suggesting they are in close contact with the substrate.

A

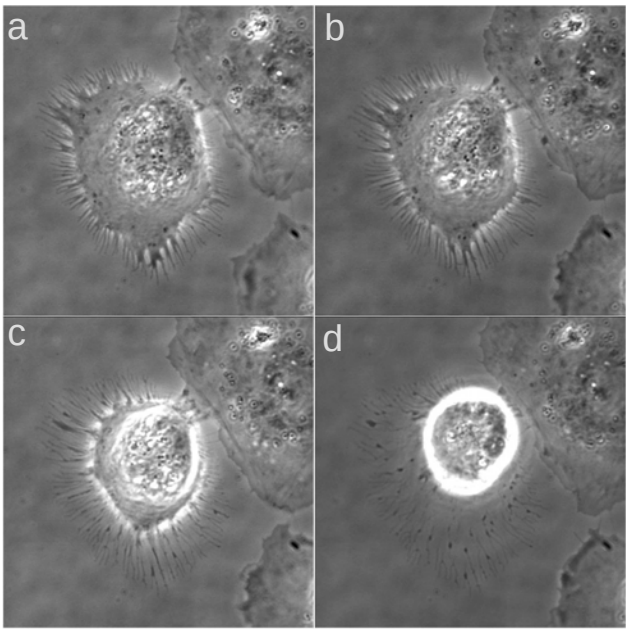

B

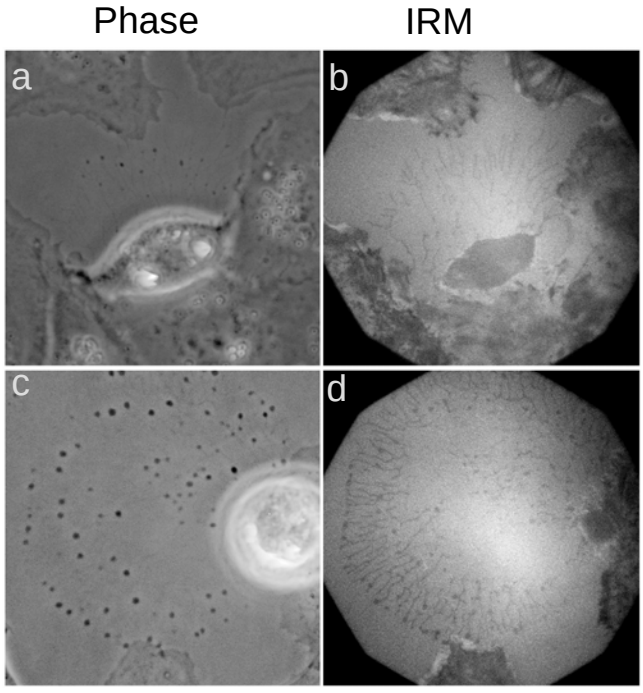

Figure 4.2 Post-mitotic spreading involves rapid expansion and extension of cytoplasm along retraction fibers toward their tips (arrowheads). Time-lapse images show filopodia-like projections (arrows). The cytoplasm appears to flow into retraction fibers and inflate them into broad expanses (Supplemental video 4.1). Plots of the speed of spreading indicate a high speed of spreading before the cell border reaches the tips of retraction fibers (average speed = 1.43±0.43μm^2/sec), and a much lower rate afterwards (0.31±0.10μm^2/sec) (n=13) (B). The spreading curves from 7 post-mitotic cells indicate that the spreading speed is faster at the early stage of post-mitotic spreading than that at the late stage of post-mitotic spreading (C).

A

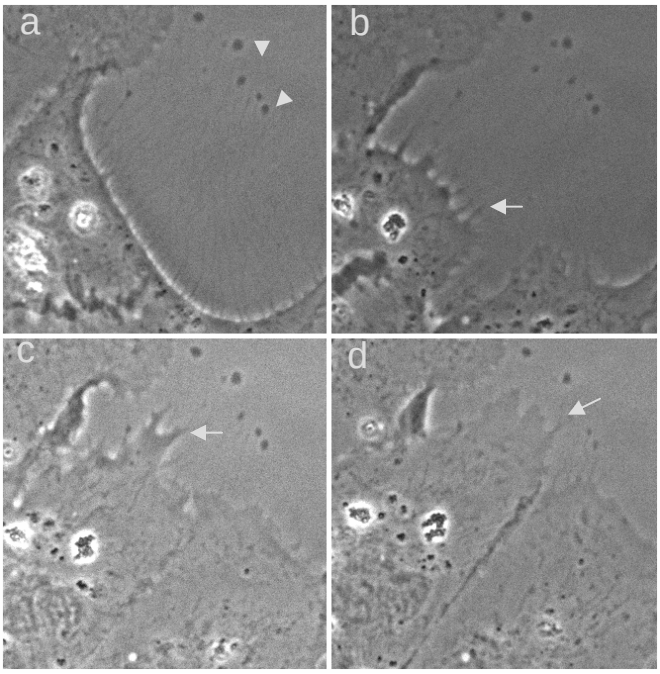
a
b
c
d

B

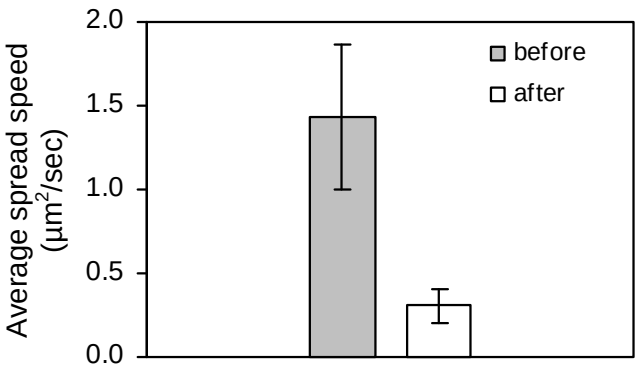
Average spread speed (μm²/sec)
2.0
1.5
1.0
0.5
0.0
before
after

C

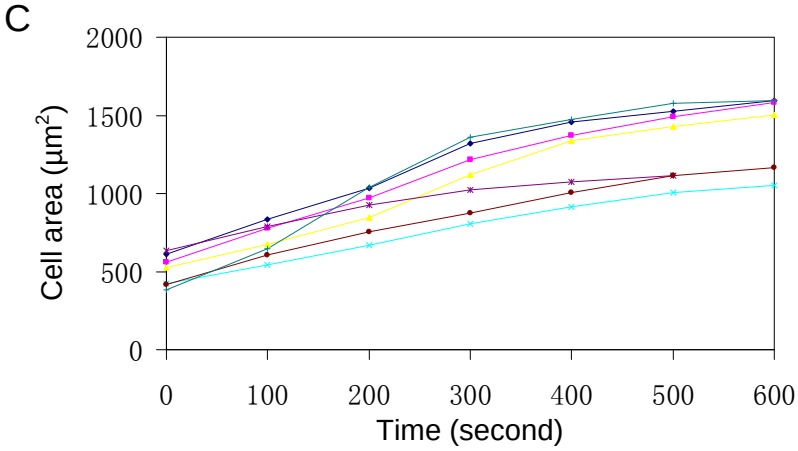
Cell area (μm²)
2000
1500
1000
500
0
0
100
200
300
400
500
600
Time (second)

mitotic spreading indicated the average spreading speed was 1.43±0.43μm^2/sec before the cell boundary reached the tips of retraction fibers, and dramatically reduced to 0.31±0.10μm^2/sec afterwards(n=13) (Figure 4.2 B). The ratio of spreading rate before and after reaching the tips of retraction fibers was 4.9±1.2 (n=13), suggesting that retraction fibers facilitate post-mitotic spreading. To find out whether the spreading speed is linear before the cell boundary reached the tips of the retraction fibers, the cell area was plotted against time every 100 seconds during a 10 minute period of time after post-mitotic spreading begins. The spreading curves indicate that the spreading speed is fast at the early stage and gradually slows down at the late stage of post-mitotic spreading (Figure 4.2C).

Retraction fibers guide the direction of post-mitotic spreading

To further understand the role of retraction fibers, I searched for mitotic cells that showed retraction fibers only on one side of the cell and neighboring cell on the other side. A microneedle was then used to remove carefully the neighboring cell without damaging the mitotic cell. Small projections were first observed along all directions during early post-mitotic spreading (Supplemental video 2). However during the subsequent spreading cells spread towards the direction with retraction fibers. The cell area on the side with retraction fibers and the side without retraction fibers was measured during a 5 minute period of time after post-mitotic spreading begins. The average spreading speed was 2.06±0.53 μm^2/sec (n=11). The spread area on the side with retraction fibers was 2.8±0.6 (n=11) times that of the side without retraction

fibers (Figure 4.3A and B), consistent with the notion that retraction fibers accelerate and/or guide the direction of post-mitotic spreading.

To further investigate the function of retraction fibers, I plated mitotic cells that were shaken off from a culture dish on fibronectin coated coverslips. These cells were able to attach and undergo mitosis, cytokinesis, and post-mitotic spreading without retraction fibers. However, their spreading speed averaged $0.35\pm0.27\mu m^2$/sec (n=9), much slower than cells with retraction fibers, and similar to that after the cell boundary reached the tip of retraction fibers during normal post-mitotic spreading (Figure 4.3C). These results further support the idea that retraction fibers facilitate post-mitotic spreading.

Figure 4.3 Retraction fibers guide the direction of post-mitotic spreading. A mitotic cell with retraction fibers on only one side of the cell (A, a, arrows) is removed of the neighboring cell on the other side (A, b, asterisk) with a microneedle. The lack of retraction fibers on the lower side is confirmed by the lack of phase-dense dots that mark the tips of retraction fibers. Post-mitotic spreading was compared in the same cell on both sides (A, c,d,e,f). The spread area on the side with retraction fibers was 2.8±0.6 (n=11) times of that on the side without retraction fibers (B). Supplemental video 4.2 shows the corresponding movie. To further compare post-mitotic spreading in different cells with or without retraction fibers, mitotic cells were shaken off and then plated on fibronectin coated coverslips. Their post-mitotic spreading speed averaged 0.35±0.27μm^2/sec (n=9), much slower than normal cells with retraction fibers (1.43±0.43μm^2/sec) (C).

A

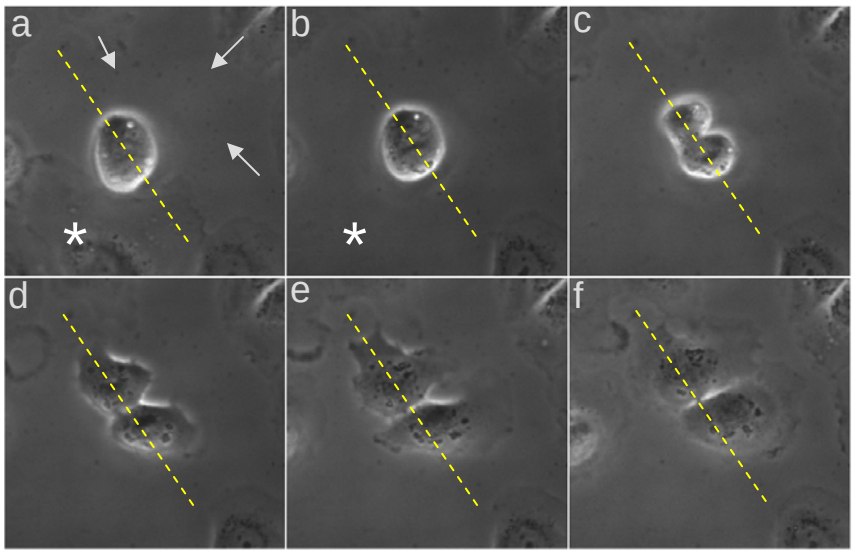
a
b
c
d
e
f

B

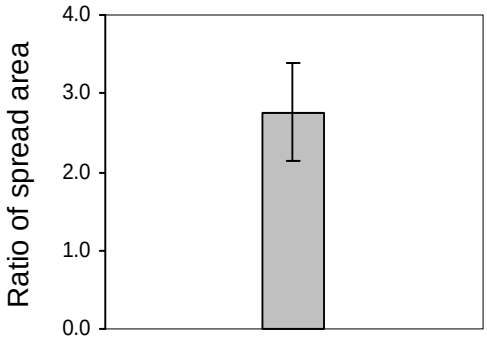
Ratio of spread area
4.0
3.0
2.0
1.0
0.0

C

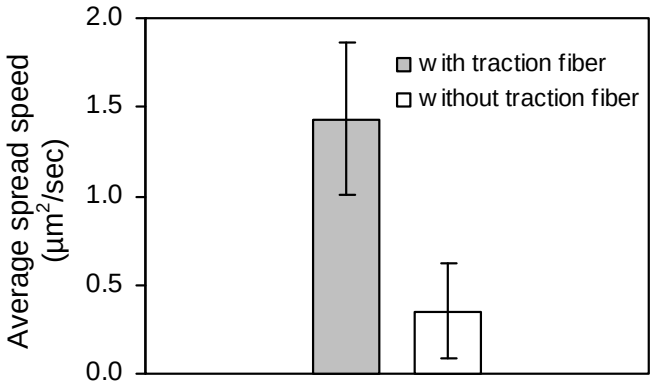
Average spread speed (μm²/sec)
2.0
1.5
1.0
0.5
0.0
with traction fiber
without traction fiber

Retraction fibers help mitotic cell reclaim its space by facilitating post-mitotic respreading

It is tempting to speculate that retraction fibers may further play a role in inhibiting the spreading of neighboring cells into the area occupied by the mitotic cell prior to mitotic rounding, similar to contact inhibition of migration. However, I found that the neighboring cells were able to move into the area covered by retraction fibers (Figure 4.4), by extending large lamellipodium over retraction fibers and overtaking the original space of the mitotic cell (Supplemental video 4.3). However, rapid respreading along retraction fibers allowed post-mitotic cells to reoccupy its previous space rapidly, forcing the neighboring cells to retreat (Figure 4.4). This result suggests that retraction fibers are involved in maintaining the space and restoring the spread morphology of post-mitotic cells.

Retraction fibers act as nucleation sites for the rapid restoration of focal adhesions during post-mitotic spreading

Mitotic rounding and post-mitotic spreading involve disassembly and reassembly of focal adhesions (Yamaguchi *et al.*, 1997; Yamakita *et al.*, 1999). As retraction fibers remain associated with the substrates, I examined their relationship to focal adhesions during post-mitotic spreading. Immunofluorescence staining of mitotic cells for focal adhesion marker proteins indicated that several focal adhesion proteins including paxillin, vinculin and zyxin are present at the tips of retraction fibers (Figure 4.5 and 4.6).

To study the dynamic process of focal adhesion reassembly during post-mitotic spreading, I took time-lapse images of RFP-zyxin expressed in motitc cells. Nascent focal

Figure 4.4 Retraction fibers cannot prevent neighboring cells from moving into the space left by mitotic cell, but help post-mitotic cells regain their space. The tips of retraction fibers are visible as phase dense dots (arrowheads). The mitotic cell and its retraction fibers are indicated by yellow circles. Large lamellipodium of neighboring cells (a,b,c, arrows) move into the space covered by retraction fibers left by mitotic cell. However, when the post-mitotic cell respreads, it quickly reoccupies its space and forces the neighboring cells to retreat (d,e, arrows), reaching the border as defined by the tips of retraction fibers. Supplemental video 4.3 shows corresponding movie.

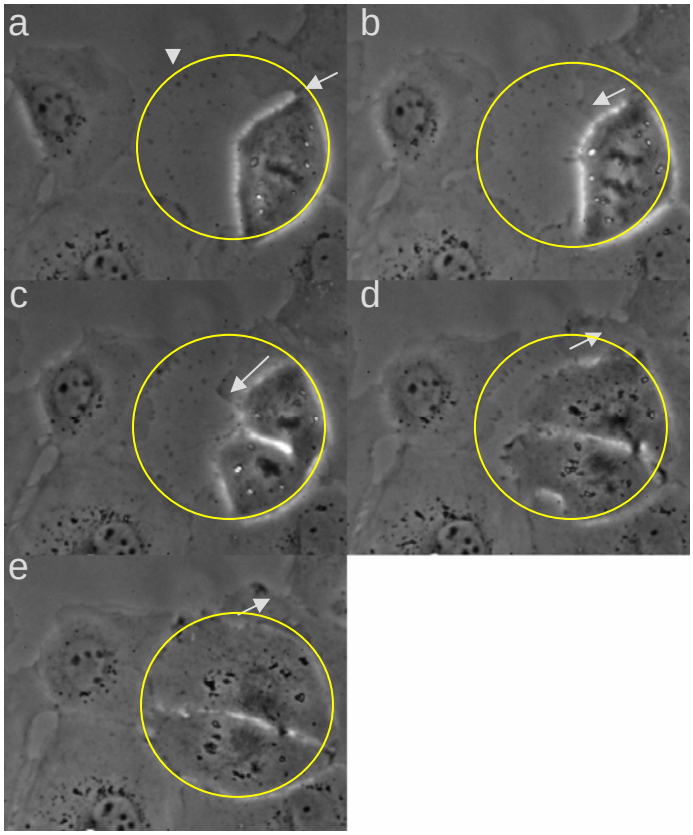
a
b
c
d
e

adhesions grew directly from zyxin dots at the tip of retraction fibers (Figure 4.6, Supplemental video 4.4), suggesting that retraction fibers may act as nucleation sites for the rapid restoration of focal adhesions and the spread interphase morphology of adherent cells. Thus unlike interphase cells where the formation of focal adhesions was coupled to protrusive activities, retraction fibers may help post-mitotic cells reassemble their adhesions through existing structures.

One question is that this study is based on cells grown on planar 2D tissue culture substrates; however, the in vivo environment is three-dimensional extracellular matrix (ECM). It's interesting to ask whether retraction fibers also exist in cells cultured in 3D matrices and whether they play a similar role. Molecular composition of 3D-matrix adhesions includes many proteins observed in 2D focal adhesions and fibrillar adhesions, such as a5-integrin, paxillin, vinculin, tensin, talin and focal adhesion kinase (FAK) (Cukierman *et al*., 2001). It is challenging to image the cell interactions with ECM in 3D matrices because of the increased depth and complexity of the 3D environment. One approach is to use two-photon microscope that permits higher resolution in 3D imaging. Another approach is to use a 3D culture system that can be imaged using conventional microscopy. In this lab we have established a 3D model by culturing cells between the gaps of two glass coverslips coated with ECM proteins (Beningo *et al*., 2004). This 3D model allows a moderately high resolution using conventional microscopy.

In conclusion, retraction fibers may provide structural support and facilitate rapid post-mitotic spreading. The function of these structures may not be limited to post-mitotic spreading, and may have broader implications in the basic mechanism of cell-

substrate interaction and cytoskeleton reorganization. The future direction is to study retraction fibers and their role in post-mitotic spreading in 3D models.

Figure 4.5 Focal adhesion proteins are concentrated at the tip of retraction fibers. The phase dense tips of retraction fibers (arrows, left panel) shows a concentration of paxillin (upper panels) or vinculin (lower panels) in immunostaining images (arrows, middle and right panels).

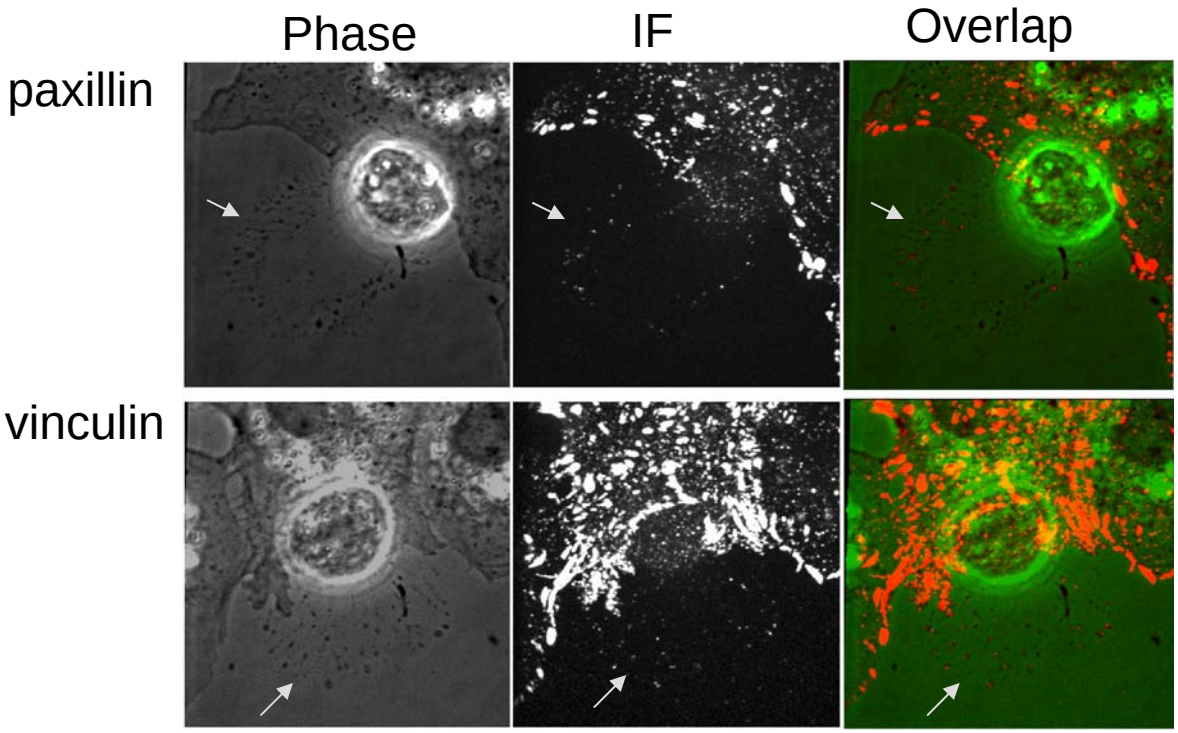
Phase
IF
Overlap
paxillin
vinculin

Figure 4.6 Focal adhesions grow directly from the tips of retraction fibers. A mitotic cell expressing RFP-zyxin shows dots of zyxin at the tip of retraction fibers (A, enlarged views of the area in yellow box over time is shown in B). Time-lapse images of RFP-zyxin show focal adhesions growing directly from the dots during post-mitotic spreading (B, arrows). Interestingly the process involves forward extension of linear structures. Supplemental video 4.4 shows corresponding movie.

A

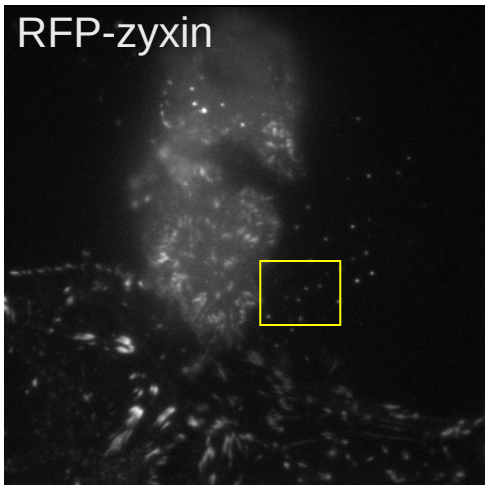

B

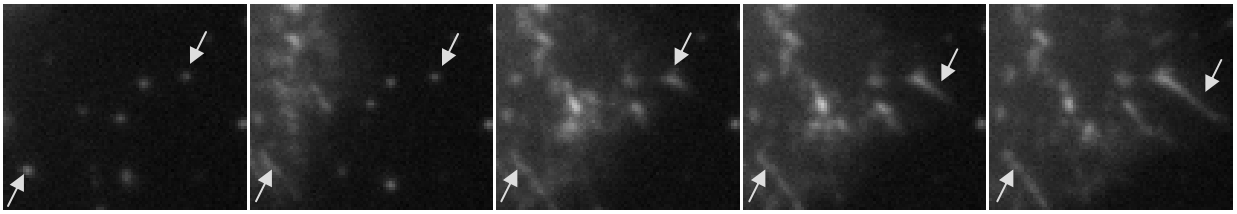

Chapter V - Discussion

Cytokinesis is a significant problem not only because it is a fundamental question in cell biology, but also because accumulating evidence indicate that defects in cytokinesis can lead to cancer and possibly other diseases (Barr and Gruneberg, 2007). The mechanism of cytokinesis has attracted the attention of cell biologists during the past two decades. While discoveries have been made, new knowledge continues to uncover new questions that need to be answered.

The main focus of this thesis is the dynamics and function of actin and myosin II during cytokinesis. The first project is to study the role of myosin II motor activity in cytokinesis using primarily drug treatment. The major conclusion is that myosin ATPase is required for actin dynamics and disassembly in the cytokinetic furrow. In addition, myosin II likely plays a global role throughout the cortex since localized inhibition of myosin II in both the furrow and polar region causes defects in cytokinesis. Interestingly, myosin II motor activity is not required for actin concentration in the furrow. These findings reveal new roles for myosin II, and raise more questions that lead to my second project.

The second project uses improved imaging techniques, the total internal fluorescence microscope (TIRF-M) to examine dorsal cortical dynamics during early cytokinesis. The quality of TIRF image is much better than that of conventional light microscopes, allowing the detection of fine cortical structures. Time-lapse sequences indicate that no cortical flow of myosin is observed on the membrane in contrast to a prominent actin flux during cytokinetic furrow assembly. Myosin II disassembly or dissociation appears to be inhibited in the equatorial region, which accounts at least

partially for its equatorial accumulation. Inhibition of myosin II motor activity inhibits actin flux but does not inhibit actin concentration in the equator, suggesting multiple mechanisms for actin recruitment to the furrow. In addition, myosin II recruitment in early cytokinesis is actin independent, while maintenance of its organization at later stage requires actin filaments.

It would be of interest to discuss these results in relation to a few published and unpublished findings. First is the dynamics of cortical myosin II during mitosis and cytokinesis. Myosin II filaments appear to cluster in small dots that associate with the membrane after cell rounds up. Although there is no long-range lateral movement, these structures appear to be very dynamic and remain in focus only for seconds to tens of seconds. It remains to be determined how they form these structures, associate with the cortex, interact with other cortical molecules, and dissociate from the membrane. In addition, while the distribution and concentration of cortical myosin II do not show obvious change from prometaphase to metaphase, the cortex becomes unstable and displays sporadic and randomly localized patches of myosin II immediately after chromosome segregation. This event is transient, subsiding quickly when a visible myosin II band appears along the equator. This observation may reflect a transition of the cortex from metaphase to anaphase, driven possibly by the localization of ring assembly signals from a diffuse distribution in the cytoplasm or cortex to the equatorial region. Such transition could be mediated by the polymerization and elongation of microtubules that eventually interact with the cortex and regulates cortical activities. A combination of local and global treatments of nocodazole or taxol may provide evidence for the role of microtubules in cortical myosin II activity.

Also of interest is that treatments with Y-27632 or Blebbistatin, both affecting myosin II activities, result in different responses. Y-27632 inhibits both myosin II phosphorylation and ATPase activity while blebbistatin only inhibits ATPase activity. It appears that Y-27632 inhibits myosin II cortical association, while blebbistatin to the contrary strengthens myosin cortical association and inhibits myosin disassembly and dissociation from the cortex. This difference demonstrates different roles of rMLC phosphorylation and ATPase in the regulation of myosin dynamics, which may be related to the folded conformation of myosin II with dephosphorylated rMLC

The second question of major interest concerns the organization of the actomyosin ring and the associated challenge in imaging the ingression process. The structure of the equatorial actomyosin ring and the mechanism of equatorial ingression are still poorly understood. TIRF-M allowed high resolution observations only during the early stage of cytokinesis, before the cell cortex becomes too far from the substrate for the evanescent wave. However, it is plausible to use TIRF-M to image the ingression process for a limited time before the dorsal cortex detaches from the substrate (unpublished observation). Additional challenges arise from the crowding of structures as the equatorial region becomes increasingly dense during ingression. Potential solutions to extend the period of observation include expressing a lower amount of proteins and to use alternative optics such as two-photon excitation, which may also address the possibility of vertical movements of the cortex. Other molecules present in the furrow cortex, such as alpha-actinin and anillin, may also serve as useful markers for imaging.

The third question of interest is the role of RhoA in cytokinesis. A puzzle is that in NRK cells injected with RhoA inhibitor C3, there is no apparent actin or myosin

concentration in the equator, yet most cells are able to elongate and cleave in the middle. What is then the mechanism that drives the ingression without a detectable contractile ring? Traction forces generated by the two daughter cells in opposite directions were suspected previously (O'Connell *et al.*, 1999). However, treatment with Y-27632 is known to cause strong inhibition of traction forces (Beningo *et al.*, 2006). While there may be residual traction forces sufficient for the ingression, other possibilities should be considered. For example, in C3 treated NRK cells, the equatorial cortex appears to be the weakest part as suggested by the weaker staining of actin filaments than other regions of the cortex. Is it possible that, in the presence of a weakened equatorial cortex, the combination of cell elongation and outward expansion of polar cortex due to post-mitotic spreading is sufficient to cause a net collapse in the middle of the cell? Could a similar mechanism play a role during normal cytokinesis? Answering these questions requires addressing another, more fundamental question: how is the cell cortex modulated and deformed upon mitotic exit. As observed in most rounded mitotic cells, the cell body first elongates before cleavage furrow appears in the middle. In addition, when using Cdk1 inhibitors to induce precocious cytokinesis in Hela cells, low doses of the drug can actually induce the elongation of the cell body without inducing cytokinesis (unpublished observation). Is it possible that polymerization of astral microtubules pushes the polar cortex outward and leads to elongation of the cell body? Different types of adherent cells should be examined to determine if such actomyosin independent ingression is a universal event.

Cytokinesis is finely regulated both spatially and temporally. Future cytokinesis study will need experiments performed at a high spatial and temporal resolution to help

understand the mechanism (Wang, 2005). New techniques of microscopy and image analysis are being developed continuously. However, few of them have been applied to cytokinesis. Future advances will likely require a combination of microscopy, micromanipulation and molecular biology.

Reference

Abercrombie, M., and Dunn, G.A. (1975). Adhesions of fibroblasts to substratum during contact inhibition observed by interference reflection microscopy. Exp Cell Res 92, 57-62.

Alberts, A.S. (2001). Identification of a carboxyl-terminal diaphanous-related formin homology protein autoregulatory domain. J Biol Chem 276, 2824-2830.

Amano, M., Ito, M., Kimura, K., Fukata, Y., Chihara, K., Nakano, T., Matsuura, Y., and Kaibuchi, K. (1996). Phosphorylation and activation of myosin by Rho-associated kinase (Rho-kinase). J Biol Chem 271, 20246-20249.

Andrews, P.D., Knatko, E., Moore, W.J., and Swedlow, J.R. (2003). Mitotic mechanics: the auroras come into view. Curr Opin Cell Biol 15, 672-683.

Axelrod, D. (2001). Total internal reflection fluorescence microscopy in cell biology. Traffic 2, 764-774.

Barr, F.A., and Gruneberg, U. (2007). Cytokinesis: placing and making the final cut. Cell 131, 847-860.

Basto, R., Lau, J., Vinogradova, T., Gardiol, A., Woods, C.G., Khodjakov, A., and Raff, J.W. (2006). Flies without centrioles. Cell 125, 1375-1386.

Bement, W.M., Benink, H.A., and von Dassow, G. (2005). A microtubule-dependent zone of active RhoA during cleavage plane specification. J Cell Biol 170, 91-101.

Beningo, K.A., Dembo, M., Wang, Y.L. (2004). Response of fibroblasts to anchorage of dorsal extracellular matrix receptors. Proc Natl Acad Sci U S A. 101(52):18024-9.

Beningo, K.A., Hamao, K., Dembo, M., Wang, Y.L., and Hosoya, H. (2006). Traction forces of fibroblasts are regulated by the Rho-dependent kinase but not by the myosin light chain kinase. Arch Biochem Biophys 456, 224-231.

Bereiter-Hahn, J., Luck, M., Miebach, T., Stelzer, H.K., and Voth, M. (1990). Spreading of trypsinized cells: cytoskeletal dynamics and energy requirements. J Cell Sci 96 (Pt 1), 171-188.

Bonaccorsi, S., Giansanti, M.G., and Gatti, M. (1998). Spindle self-organization and cytokinesis during male meiosis in asterless mutants of Drosophila melanogaster. J Cell Biol 142, 751-761.

Bray, D., and White, J.G. (1988). Cortical Flow in Animal-Cells. Science 239, 883-888.
Bresnick, A.R. (1999). Molecular mechanisms of nonmuscle myosin-II regulation. Curr Opin Cell Biol 11, 26-33.

Bringmann, H., and Hyman, A.A. (2005). A cytokinesis furrow is positioned by two consecutive signals. Nature 436, 731-734.

Burgess, D.R., and Chang, F. (2005). Site selection for the cleavage furrow at cytokinesis. Trends Cell Biol 15, 156-162.

Burkard, M.E., Randall, C.L., Larochelle, S., Zhang, C., Shokat, K.M., Fisher, R.P., and Jallepalli, P.V. (2007). Chemical genetics reveals the requirement for Polo-like kinase 1 activity in positioning RhoA and triggering cytokinesis in human cells. Proc Natl Acad Sci U S A 104, 4383-4388.

Canman, J.C., Cameron, L.A., Maddox, P.S., Straight, A., Tirnauer, J.S., Mitchison, T.J., Fang, G., Kapoor, T.M., and Salmon, E.D. (2003). Determining the position of the cell division plane. Nature 424, 1074-1078.

Cao, L.G., and Wang, Y.L. (1990a). Mechanism of the formation of contractile ring in dividing cultured animal cells. I. Recruitment of preexisting actin filaments into the cleavage furrow. J Cell Biol 110, 1089-1095.

Cao, L.G., and Wang, Y.L. (1990b). Mechanism of the formation of contractile ring in dividing cultured animal cells. II. Cortical movement of microinjected actin filaments. J Cell Biol 111, 1905-1911.

Cao, L.G., and Wang, Y.L. (1996). Signals from the spindle midzone are required for the stimulation of cytokinesis in cultured epithelial cells. Mol Biol Cell 7, 225-232.

Castrillon, D.H., and Wasserman, S.A. (1994). Diaphanous is required for cytokinesis in Drosophila and shares domains of similarity with the products of the limb deformity gene. Development 120, 3367-3377.

Chang, F., Drubin, D., and Nurse, P. (1997). cdc12p, a protein required for cytokinesis in fission yeast, is a component of the cell division ring and interacts with profilin. J Cell Biol 137, 169-182.

Chen, W.T. (1981). Mechanism of retraction of the trailing edge during fibroblast movement. J Cell Biol 90, 187-200.

Chew, T.L., Wolf, W.A., Gallagher, P.J., Matsumura, F., and Chisholm, R.L. (2002). A fluorescent resonant energy transfer-based biosensor reveals transient and regional myosin light chain kinase activation in lamella and cleavage furrows. J Cell Biol 156, 543-553.

Conti, M.A., Even-Ram, S., Liu, C., Yamada, K.M., and Adelstein, R.S. (2004). Defects in cell adhesion and the visceral endoderm following ablation of nonmuscle myosin heavy chain II-A in mice. J Biol Chem 279, 41263-41266.

Cramer, L.P., and Mitchison, T.J. (1995). Myosin is involved in postmitotic cell spreading. J Cell Biol 131, 179-189.

Cukierman, E., Pankov, R., Stevens, D.R., and Yamada, K.M. (2001). Taking cell-matrix adhesions to the third dimension. Science 294, 1708.

Dean, S.O., Rogers, S.L., Stuurman, N., Vale, R.D., and Spudich, J.A. (2005). Distinct pathways control recruitment and maintenance of myosin II at the cleavage furrow during cytokinesis. Proc Natl Acad Sci U S A 102, 13473-13478.

Dean, S.O., and Spudich, J.A. (2006). Rho kinase's role in myosin recruitment to the equatorial cortex of mitotic Drosophila S2 cells is for myosin regulatory light chain phosphorylation. PLoS ONE 1, e131.

DeBiasio, R.L., LaRocca, G.M., Post, P.L., and Taylor, D.L. (1996). Myosin II transport, organization, and phosphorylation: evidence for cortical flow/solation-contraction coupling during cytokinesis and cell locomotion. Mol Biol Cell 7, 1259-1282.

Dobbelaere, J., and Barral, Y. (2004). Spatial coordination of cytokinetic events by compartmentalization of the cell cortex. Science 305, 393-396.

Drechsel, D.N., Hyman, A.A., Hall, A., and Glotzer, M. (1997). A requirement for Rho and Cdc42 during cytokinesis in Xenopus embryos. Curr Biol 7, 12-23.

Earnshaw, W.C., and Cooke, C.A. (1991). Analysis of the distribution of the INCENPs throughout mitosis reveals the existence of a pathway of structural changes in the chromosomes during metaphase and early events in cleavage furrow formation. J Cell Sci 98 (Pt 4), 443-461.

Echard, A., Hickson, G.R., Foley, E., and O'Farrell, P.H. (2004). Terminal cytokinesis events uncovered after an RNAi screen. Curr Biol 14, 1685-1693.

Eckley, D.M., Ainsztein, A.M., Mackay, A.M., Goldberg, I.G., and Earnshaw, W.C. (1997). Chromosomal proteins and cytokinesis: patterns of cleavage furrow formation and inner centromere protein positioning in mitotic heterokaryons and mid-anaphase cells. J Cell Biol 136, 1169-1183.

Eggert, U.S., Mitchison, T.J., and Field, C.M. (2006). Animal cytokinesis: from parts list to mechanisms. Annu Rev Biochem 75, 543-566.

Even-Ram, S., Doyle, A.D., Conti, M.A., Matsumoto, K., Adelstein, R.S., and Yamada, K.M. (2007). Myosin IIA regulates cell motility and actomyosin-microtubule crosstalk. Nat Cell Biol 9, 299-309.

Feierbach, B., and Chang, F. (2001). Cytokinesis and the contractile ring in fission yeast. Curr Opin Microbiol 4, 713-719.

Fishkind, D.J., and Wang, Y.L. (1993). Orientation and three-dimensional organization of actin filaments in dividing cultured cells. J Cell Biol 123, 837-848.

Fishkind, D.J., and Wang, Y.L. (1995). New horizons for cytokinesis. Curr Opin Cell Biol 7, 23-31.

Fukata, Y., Amano, M., and Kaibuchi, K. (2001). Rho-Rho-kinase pathway in smooth muscle contraction and cytoskeletal reorganization of non-muscle cells. Trends Pharmacol Sci 22, 32-39.

Gallagher, P.J., Herring, B.P., Griffin, S.A., and Stull, J.T. (1991). Molecular characterization of a mammalian smooth muscle myosin light chain kinase. J Biol Chem 266, 23936-23944.

Gerisch, G., and Weber, I. (2000). Cytokinesis without myosin II. Curr Opin Cell Biol 12, 126-132.

Glotzer, M. (2003). Cytokinesis: progress on all fronts. Curr Opin Cell Biol 15, 684-690.

Glotzer, M. (2005). The molecular requirements for cytokinesis. Science 307, 1735-1739.

Golomb, E., Ma, X., Jana, S.S., Preston, Y.A., Kawamoto, S., Shoham, N.G., Goldin, E., Conti, M.A., Sellers, J.R., and Adelstein, R.S. (2004). Identification and characterization of nonmuscle myosin II-C, a new member of the myosin II family. J Biol Chem 279, 2800-2808.

Goode, B.L., and Eck, M.J. (2007). Mechanism and function of formins in the control of actin assembly. Annu Rev Biochem 76, 593-627.

Gruneberg, U., Neef, R., Honda, R., Nigg, E.A., and Barr, F.A. (2004). Relocation of Aurora B from centromeres to the central spindle at the metaphase to anaphase transition requires MKlp2. J Cell Biol 166, 167-172.

Guha, M., Zhou, M., and Wang, Y.L. (2005). Cortical actin turnover during cytokinesis requires myosin II. Curr Biol 15, 732-736.

Gunsalus, K.C., Bonaccorsi, S., Williams, E., Verni, F., Gatti, M., and Goldberg, M.L. (1995). Mutations in twinstar, a Drosophila gene encoding a cofilin/ADF homologue, result in defects in centrosome migration and cytokinesis. J Cell Biol 131, 1243-1259.

Guse, A., Mishima, M., and Glotzer, M. (2005). Phosphorylation of ZEN-4/MKLP1 by aurora B regulates completion of cytokinesis. Curr Biol 15, 778-786.

Harris, A. (1973). Location of cellular adhesions to solid substrata. Dev Biol 35, 97-114.

He, X., and Dembo, M. (1997). On the mechanics of the first cleavage division of the sea urchin egg. Exp Cell Res 233, 252-273.

Hiramoto, Y. (1971). Analysis of cleavage stimulus by means of micromanipulation of sea urchin eggs. Exp Cell Res 68, 291-298.

Hird, S.N., and White, J.G. (1993). Cortical and cytoplasmic flow polarity in early embryonic cells of Caenorhabditis elegans. J Cell Biol 121, 1343-1355.

Hou, M.C., and McCollum, D. (2002). Cytokinesis: myosin spots the ring. Curr Biol 12, R334-336.

Hudson, A.M., and Cooley, L. (2002). A subset of dynamic actin rearrangements in Drosophila requires the Arp2/3 complex. J Cell Biol 156, 677-687.

Ikebe, M., Koretz, J., and Hartshorne, D.J. (1988). Effects of phosphorylation of light chain residues threonine 18 and serine 19 on the properties and conformation of smooth muscle myosin. J Biol Chem 263, 6432-6437.

Imamura, H., Tanaka, K., Hihara, T., Umikawa, M., Kamei, T., Takahashi, K., Sasaki, T., and Takai, Y. (1997). Bni1p and Bnr1p: downstream targets of the Rho family small G-proteins which interact with profilin and regulate actin cytoskeleton in Saccharomyces cerevisiae. Embo J 16, 2745-2755.

Ingouff, M., Fitz Gerald, J.N., Guerin, C., Robert, H., Sorensen, M.B., Van Damme, D., Geelen, D., Blanchoin, L., and Berger, F. (2005). Plant formin AtFH5 is an evolutionarily conserved actin nucleator involved in cytokinesis. Nat Cell Biol 7, 374-380.

Jantsch-Plunger, V., Gonczy, P., Romano, A., Schnabel, H., Hamill, D., Schnabel, R., Hyman, A.A., and Glotzer, M. (2000). CYK-4: A Rho family gtpase activating protein (GAP) required for central spindle formation and cytokinesis. J Cell Biol 149, 1391-1404.

Jiang, W., Jimenez, G., Wells, N.J., Hope, T.J., Wahl, G.M., Hunter, T., and Fukunaga, R. (1998). PRC1: a human mitotic spindle-associated CDK substrate protein required for cytokinesis. Mol Cell 2, 877-885.

Jordan, P., and Karess, R. (1997). Myosin light chain-activating phosphorylation sites are required for oogenesis in Drosophila. J Cell Biol 139, 1805-1819.

Kamasaki, T., Osumi, M., and Mabuchi, I. (2007). Three-dimensional arrangement of F-actin in the contractile ring of fission yeast. J Cell Biol 178, 765-771.

Kimura, K., Ito, M., Amano, M., Chihara, K., Fukata, Y., Nakafuku, M., Yamamori, B., Feng, J., Nakano, T., Okawa, K., Iwamatsu, A., and Kaibuchi, K. (1996). Regulation of myosin phosphatase by Rho and Rho-associated kinase (Rho-kinase). Science 273, 245-248.

Kirfel, G., Rigort, A., Borm, B., Schulte, C., and Herzog, V. (2003). Structural and compositional analysis of the keratinocyte migration track. Cell Motil Cytoskeleton 55, 1-13.

Kishi, K., Sasaki, T., Kuroda, S., Itoh, T., and Takai, Y. (1993). Regulation of cytoplasmic division of Xenopus embryo by rho p21 and its inhibitory GDP/GTP exchange protein (rho GDI). J Cell Biol 120, 1187-1195.

Kolega, J. (1998). Cytoplasmic dynamics of myosin IIA and IIB: spatial 'sorting' of isoforms in locomoting cells. J Cell Sci 111 (Pt 15), 2085-2095.

Kolega, J. (2004). Phototoxicity and photoinactivation of blebbistatin in UV and visible light. Biochem Biophys Res Commun 320, 1020-1025.

Komatsu, S., Yano, T., Shibata, M., Tuft, R.A., and Ikebe, M. (2000). Effects of the regulatory light chain phosphorylation of myosin II on mitosis and cytokinesis of mammalian cells. J Biol Chem 275, 34512-34520.

Kosako, H., Yoshida, T., Matsumura, F., Ishizaki, T., Narumiya, S., and Inagaki, M. (2000). Rho-kinase/ROCK is involved in cytokinesis through the phosphorylation of myosin light chain and not ezrin/radixin/moesin proteins at the cleavage furrow. Oncogene 19, 6059-6064.

Kunda, P., Pelling, A.E., Liu, T., and Baum, B. (2008). Moesin controls cortical rigidity, cell rounding, and spindle morphogenesis during mitosis. Curr Biol 18, 91-101.

Lauffenburger, D.A., and Horwitz, A.F. (1996). Cell migration: a physically integrated molecular process. Cell 84, 359-369.

Lowery, D.M., Clauser, K.R., Hjerrild, M., Lim, D., Alexander, J., Kishi, K., Ong, S.E., Gammeltoft, S., Carr, S.A., and Yaffe, M.B. (2007). Proteomic screen defines the Polo-box domain interactome and identifies Rock2 as a Plk1 substrate. Embo J 26, 2262-2273.

Lucero, A., Stack, C., Bresnick, A.R., and Shuster, C.B. (2006) A global myosin light chain kinase-dependent increase in myosin II contractility accompanies the metaphase-anaphase transition in sea urchin eggs. Mol Biol Cell 17, 4093-4104.

Mabuchi, I., Hamaguchi, Y., Fujimoto, H., Morii, N., Mishima, M., and Narumiya, S. (1993). A rho-like protein is involved in the organisation of the contractile ring in dividing sand dollar eggs. Zygote 1, 325-331.

Madaule, P., Eda, M., Watanabe, N., Fujisawa, K., Matsuoka, T., Bito, H., Ishizaki, T., and Narumiya, S. (1998). Role of citron kinase as a target of the small GTPase Rho in cytokinesis. Nature 394, 491-494.

Matsumura, F. (2005). Regulation of myosin II during cytokinesis in higher eukaryotes. Trends Cell Biol 15, 371-377.

Matzke, R., Jacobson, K., and Radmacher, M. (2001). Direct, high-resolution measurement of furrow stiffening during division of adherent cells. Nat Cell Biol 3, 607-610.

Maupin, P., Phillips, C.L., Adelstein, R.S., and Pollard, T.D. (1994). Differential localization of myosin-II isozymes in human cultured cells and blood cells. J Cell Sci 107 (Pt 11), 3077-3090.

McCollum, D. (2004). Cytokinesis: the central spindle takes center stage. Curr Biol 14, R953-955.

McKenna, N.M., and Wang, Y.L. (1989). Culturing cells on the microscope stage. Methods Cell Biol 29, 195-205.

Minoshima, Y., Kawashima, T., Hirose, K., Tonozuka, Y., Kawajiri, A., Bao, Y.C., Deng, X., Tatsuka, M., Narumiya, S., May, W.S., Jr., Nosaka, T., Semba, K., Inoue, T., Satoh, T., Inagaki, M., and Kitamura, T. (2003). Phosphorylation by aurora B converts MgcRacGAP to a RhoGAP during cytokinesis. Dev Cell 4, 549-560.

Mishima, M., Pavicic, V., Gruneberg, U., Nigg, E.A., and Glotzer, M. (2004). Cell cycle regulation of central spindle assembly. Nature 430, 908-913.

Mollinari, C., Kleman, J.P., Jiang, W., Schoehn, G., Hunter, T., and Margolis, R.L. (2002). PRC1 is a microtubule binding and bundling protein essential to maintain the mitotic spindle midzone. J Cell Biol 157, 1175-1186.

Mollinari, C., Kleman, J.P., Saoudi, Y., Jablonski, S.A., Perard, J., Yen, T.J., and Margolis, R.L. (2005). Ablation of PRC1 by small interfering RNA demonstrates that cytokinetic abscission requires a central spindle bundle in mammalian cells, whereas completion of furrowing does not. Mol Biol Cell 16, 1043-1055.

Moussavi, R.S., Kelley, C.A., and Adelstein, R.S. (1993). Phosphorylation of vertebrate nonmuscle and smooth muscle myosin heavy chains and light chains. Mol Cell Biochem 127-128, 219-227.

Mukhina, S., Wang, Y.L., and Murata-Hori, M. (2007). Alpha-actinin is required for tightly regulated remodeling of the actin cortical network during cytokinesis. Dev Cell 13, 554-565.

Murthy, K., and Wadsworth, P. (2005). Myosin-II-dependent localization and dynamics of F-actin during cytokinesis. Curr Biol 15, 724-731.

Naim, V., Imarisio, S., Di Cunto, F., Gatti, M., and Bonaccorsi, S. (2004). Drosophila citron kinase is required for the final steps of cytokinesis. Mol Biol Cell 15, 5053-5063.

Nislow, C., Lombillo, V.A., Kuriyama, R., and McIntosh, J.R. (1992). A plus-end-directed motor enzyme that moves antiparallel microtubules in vitro localizes to the interzone of mitotic spindles. Nature 359, 543-547.

Noguchi, T., and Mabuchi, I. (2001). Reorganization of actin cytoskeleton at the growing end of the cleavage furrow of Xenopus egg during cytokinesis. J Cell Sci 114, 401-412.

O'Connell, C.B., Warner, A.K., and Wang, Y. (2001). Distinct roles of the equatorial and polar cortices in the cleavage of adherent cells. Curr Biol 11, 702-707.

O'Connell, C.B., Wheatley, S.P., Ahmed, S., and Wang, Y.L. (1999). The small GTP-binding protein rho regulates cortical activities in cultured cells during division. J Cell Biol 144, 305-313.

Oegema, K., Savoian, M.S., Mitchison, T.J., and Field, C.M. (2000). Functional analysis of a human homologue of the Drosophila actin binding protein anillin suggests a role in cytokinesis. J Cell Biol 150, 539-552.

Pelham, R.J., and Chang, F. (2002). Actin dynamics in the contractile ring during cytokinesis in fission yeast. Nature 419, 82-86.

Pereira, G., and Schiebel, E. (2003). Separase regulates INCENP-Aurora B anaphase spindle function through Cdc14. Science 302, 2120-2124.

Petronczki, M., Glotzer, M., Kraut, N., and Peters, J.M. (2007). Polo-like kinase 1 triggers the initiation of cytokinesis in human cells by promoting recruitment of the RhoGEF Ect2 to the central spindle. Dev Cell 12, 713-725.

Phillips, C.L., Yamakawa, K., and Adelstein, R.S. (1995). Cloning of the cDNA encoding human nonmuscle myosin heavy chain-B and analysis of human tissues with isoform-specific antibodies. J Muscle Res Cell Motil 16, 379-389.

Piekny, A., Werner, M., and Glotzer, M. (2005). Cytokinesis: welcome to the Rho zone. Trends Cell Biol 15, 651-658.

Piekny, A.J., and Mains, P.E. (2002). Rho-binding kinase (LET-502) and myosin phosphatase (MEL-11) regulate cytokinesis in the early Caenorhabditis elegans embryo. J Cell Sci 115, 2271-2282.

Potapova, T.A., Daum, J.R., Pittman, B.D., Hudson, J.R., Jones, T.N., Satinover, D.L., Stukenberg, P.T., and Gorbsky, G.J. (2006). The reversibility of mitotic exit in vertebrate cells. Nature 440, 954-958.

Prokopenko, S.N., Brumby, A., O'Keefe, L., Prior, L., He, Y., Saint, R., and Bellen, H.J. (1999). A putative exchange factor for Rho1 GTPase is required for initiation of cytokinesis in Drosophila. Genes Dev 13, 2301-2314.

Rappaport, R. (1961). Experiments concerning the cleavage stimulus in sand dollar eggs. J Exp Zool 148, 81-89.

Rappaport, R. (1967). Cell division: direct measurement of maximum tension exerted by furrow of echinoderm eggs. Science 156, 1241-1243.

Rappaport, R. (1968). [Geometrical relations of the cleavage stimulus in flattened, perforated sea urchin eggs]. Embryologia (Nagoya) 10, 89-104.

Rappaport, R. (1996). Cytokinesis in Animal Cells. Cambridge: Cambridge University Press.

Rappaport, R., Jr. (1960). Cleavage of sand dollar eggs under constant tensile stress. J Exp Zool 144, 225-231.

Richter, E., Hitzler, H., Zimmermann, H., Hagedorn, R., and Fuhr, G. (2000). Trace formation during locomotion of L929 mouse fibroblasts continuously recorded by interference reflection microscopy (IRM). Cell Motil Cytoskeleton 47, 38-47.

Robinson, D.N., Cavet, G., Warrick, H.M., and Spudich, J.A. (2002). Quantitation of the distribution and flux of myosin-II during cytokinesis. BMC Cell Biol 3, 4.

Royou, A., Sullivan, W., and Karess, R. (2002). Cortical recruitment of nonmuscle myosin II in early syncytial Drosophila embryos: its role in nuclear axial expansion and its regulation by Cdc2 activity. J Cell Biol 158, 127-137.

Ruchaud, S., Carmena, M., and Earnshaw, W.C. (2007). Chromosomal passengers: conducting cell division. Nat Rev Mol Cell Biol 8, 798-812.

Satterwhite, L.L., and Pollard, T.D. (1992). Cytokinesis. Curr Opin Cell Biol 4, 43-52.

Scholey, J.M., Taylor, K.A., and Kendrick-Jones, J. (1980). Regulation of non-muscle myosin assembly by calmodulin-dependent light chain kinase. Nature 287, 233-235.

Schroeder, T.E. (1972). The contractile ring. II. Determining its brief existence, volumetric changes, and vital role in cleaving Arbacia eggs. J Cell Biol 53, 419-434.

Severson, A.F., Baillie, D.L., and Bowerman, B. (2002). A Formin Homology protein and a profilin are required for cytokinesis and Arp2/3-independent assembly of cortical microfilaments in C. elegans. Curr Biol 12, 2066-2075.

Severson, A.F., and Bowerman, B. (2003). Myosin and the PAR proteins polarize microfilament-dependent forces that shape and position mitotic spindles in Caenorhabditis elegans. J Cell Biol 161, 21-26.

Shannon, K.B., Canman, J.C., Ben Moree, C., Tirnauer, J.S., and Salmon, E.D. (2005). Taxol-stabilized microtubules can position the cytokinetic furrow in mammalian cells. Mol Biol Cell 16, 4423-4436.

Sheetz, M.P., Felsenfeld, D., Galbraith, C.G., and Choquet, D. (1999). Cell migration as a five-step cycle. Biochem Soc Symp 65, 233-243.

Simons, M., Wang, M., McBride, O.W., Kawamoto, S., Yamakawa, K., Gdula, D., Adelstein, R.S., and Weir, L. (1991). Human nonmuscle myosin heavy chains are encoded by two genes located on different chromosomes. Circ Res 69, 530-539.

Straight, A.F., Cheung, A., Limouze, J., Chen, I., Westwood, N.J., Sellers, J.R., and Mitchison, T.J. (2003). Dissecting temporal and spatial control of cytokinesis with a myosin II Inhibitor. Science 299, 1743-1747.

Straight, A.F., Field, C.M., and Mitchison, T.J. (2005). Anillin binds nonmuscle myosin II and regulates the contractile ring. Mol Biol Cell 16, 193-201.

Strickland, L.I., Donnelly, E.J., and Burgess, D.R. (2005). Induction of cytokinesis is independent of precisely regulated microtubule dynamics. Mol Biol Cell 16, 4485-4494.

Takeda, K., Kishi, H., Ma, X., Yu, Z.X., and Adelstein, R.S. (2003). Ablation and mutation of nonmuscle myosin heavy chain II-B results in a defect in cardiac myocyte cytokinesis. Circ Res 93, 330-337.

Tatsumoto, T., Xie, X., Blumenthal, R., Okamoto, I., and Miki, T. (1999). Human ECT2 is an exchange factor for Rho GTPases, phosphorylated in G2/M phases, and involved in cytokinesis. J Cell Biol 147, 921-928.

Tolliday, N., VerPlank, L., and Li, R. (2002). Rho1 directs formin-mediated actin ring assembly during budding yeast cytokinesis. Curr Biol 12, 1864-1870.

Uehara, R., Hosoya, H., and Mabuchi, I. (2008). In vivo phosphorylation of regulatory light chain of myosin II in sea urchin eggs and its role in controlling myosin localization and function during cytokinesis. Cell Motil Cytoskeleton 65, 100-115.

Uyeda, T.Q., and Nagasaki, A. (2004). Variations on a theme: the many modes of cytokinesis. Curr Opin Cell Biol 16, 55-60.

Uyeda, T.Q., Nagasaki, A., and Yumura, S. (2004). Multiple parallelisms in animal cytokinesis. Int Rev Cytol 240, 377-432.

Vader, G., Medema, R.H., and Lens, S.M. (2006). The chromosomal passenger complex: guiding Aurora-B through mitosis. J Cell Biol 173, 833-837.

Verkhovsky, A.B., and Borisy, G.G. (1993). Non-sarcomeric mode of myosin II organization in the fibroblast lamellum. J Cell Biol 123, 637-652.

Wang, Y.-L. (1992). Fluorescence microscopic analysis of cytoskeletal organization and dynamics. In: Cytoskeleton: A Practical Approach, ed. K.L.C.a.C.A.C. Carraway, Oxford: Oxford University Press, 1-22.

Wang, Y.L. (2005). The mechanism of cortical ingression during early cytokinesis: thinking beyond the contractile ring hypothesis. Trends Cell Biol 15, 581-588.

Wang, Y.L., Silverman, J.D., and Cao, L.G. (1994). Single particle tracking of surface receptor movement during cell division. J Cell Biol 127, 963-971.

Watanabe, N., Kato, T., Fujita, A., Ishizaki, T., and Narumiya, S. (1999). Cooperation between mDia1 and ROCK in Rho-induced actin reorganization. Nat Cell Biol 1, 136-143.

Werner, M., Munro, E., and Glotzer, M. (2007). Astral signals spatially bias cortical Myosin recruitment to break symmetry and promote cytokinesis. Curr Biol 17, 1286-1297.

Wheatley, S.P., and Wang, Y. (1996). Midzone microtubule bundles are continuously required for cytokinesis in cultured epithelial cells. J Cell Biol 135, 981-989.

White, J.G., and Borisy, G.G. (1983). On the mechanisms of cytokinesis in animal cells. J Theor Biol 101, 289-316.

Wolf, K., Mazo, I., Leung, H., Engelke, K., von Andrian, U.H., Deryugina, E.I., Strongin, A.Y., Brocker, E.B., and Friedl, P. (2003). Compensation mechanism in tumor cell migration: mesenchymal-amoeboid transition after blocking of pericellular proteolysis. J Cell Biol 160, 267-277.

Wolfe, B.A., and Gould, K.L. (2005). Split decisions: coordinating cytokinesis in yeast. Trends Cell Biol 15, 10-18.

Yamaguchi, R., Mazaki, Y., Hirota, K., Hashimoto, S., and Sabe, H. (1997). Mitosis specific serine phosphorylation and downregulation of one of the focal adhesion protein, paxillin. Oncogene 15, 1753-1761.

Yamakita, Y., Totsukawa, G., Yamashiro, S., Fry, D., Zhang, X., Hanks, S.K., and Matsumura, F. (1999). Dissociation of FAK/p130(CAS)/c-Src complex during mitosis: role of mitosis-specific serine phosphorylation of FAK. J Cell Biol 144, 315-324.

Yamashiro, S., Totsukawa, G., Yamakita, Y., Sasaki, Y., Madaule, P., Ishizaki, T., Narumiya, S., and Matsumura, F. (2003). Citron kinase, a Rho-dependent kinase, induces di-phosphorylation of regulatory light chain of myosin II. Mol Biol Cell 14, 1745-1756.

Yamashiro, S., Yamakita, Y., Totsukawa, G., Goto, H., Kaibuchi, K., Ito, M., Hartshorne, D.J., and Matsumura, F. (2008). Myosin phosphatase-targeting subunit 1 regulates mitosis by antagonizing polo-like kinase 1. Dev Cell 14, 787-797.

Yuce, O., Piekny, A., and Glotzer, M. (2005). An ECT2-centralspindlin complex regulates the localization and function of RhoA. J Cell Biol 170, 571-582.

Yumura, S. (2001). Myosin II dynamics and cortical flow during contractile ring formation in Dictyostelium cells. J Cell Biol 154, 137-146.

Yumura, S., and Uyeda, T.Q. (1997). Transport of myosin II to the equatorial region without its own motor activity in mitotic Dictyostelium cells. Mol Biol Cell 8, 2089-2099.

Zang, J.H., and Spudich, J.A. (1998). Myosin II localization during cytokinesis occurs by a mechanism that does not require its motor domain. Proc Natl Acad Sci U S A 95, 13652-13657.

Zhou, M., and Wang, Y.L. (2008). Distinct pathways for the early recruitment of myosin II and actin to the cytokinetic furrow. Mol Biol Cell 19, 318-326.

Zimmermann, H., Hagedorn, R., Richter, E., and Fuhr, G. (1999). Topography of cell traces studied by atomic force microscopy. Eur Biophys J 28, 516-525.